NOAA Technical Memorandum NMFS-AFSC-507

Results of the Acoustic-Trawl Survey of Walleye Pollock (*Gadus chalcogrammus*) in the Eastern Bering Sea, June-August 2024 (DY2024-08)

A. McCarthy, T. Honkalehto, and N. Lauffenburger

January 2026

U.S. DEPARTMENT OF COMMERCE

National Oceanic and Atmospheric Administration
National Marine Fisheries Service
Alaska Fisheries Science Center

This document should be cited as follows:

McCarthy, A., Honkalehto, T., and Lauffenburger, N. 2026. Results of the acoustic-trawl survey of walleye pollock (*Gadus chalcogrammus*) in the eastern Bering Sea, June-August 2024 (DY2024-08). U.S. Department of Commerce, NOAA Technical Memorandum NMFS-AFSC-507, 68 p.

This document is available online at:

Document available: https://repository.library.noaa.gov

Results of the Acoustic-Trawl Survey of Walleye Pollock (*Gadus chalcogrammus*) in the Eastern Bering Sea, June-August 2024 (DY2024-08)

A. McCarthy, T. Honkalehto, and N. Lauffenburger

Resource Assessment and Conservation Engineering Division
Alaska Fisheries Science Center
National Marine Fisheries Service
National Oceanic and Atmospheric Administration
7600 Sand Point Way NE
Seattle, WA 98115

U.S. DEPARTMENT OF COMMERCE

National Oceanic and Atmospheric Administration
National Marine Fisheries Service
Alaska Fisheries Science Center

NOAA Technical Memorandum NMFS-TM-AFSC-507

January 2026

ABSTRACT

Eastern Bering Sea (EBS) shelf walleye pollock (*Gadus chalcogrammus*; hereafter "pollock") midwater abundance and distribution were assessed from Bristol Bay to the U.S.-Russia Convention Line from 11 June to 18 July 2024 using acoustic-trawl (AT) survey methods aboard the NOAA Ship *Oscar Dyson*. Previous surveys of the EBS have been regularly conducted by the Midwater Assessment and Conservation Engineering (MACE) Program since 1979. In 2024, pollock biomass was concentrated between the 100 m isobath and the shelf break, particularly in the Bering Canyon north of Unimak Pass and between Zhemchug Canyon and the U.S.-Russia Convention Line. The estimated abundance of pollock in midwater (between 16.0 m from the sea surface and 0.5 m off the seafloor) in the core survey area was 11.4 billion fish weighing 2.9 million metric tons (t). This represents a 1.2% increase in numbers of fish and a 32.9% decrease in biomass from the 2022 estimated abundance. The majority of the pollock biomass was observed west of 170 °W (62.1%). Age-6 pollock dominated by weight, and age-1 pollock dominated numerically: 47.7% of the total pollock biomass was attributed to age-6 fish, and 44.5% of the total pollock numbers was attributed to age-1 fish.

Sea surface temperatures (SST) were cooler in 2024 (mean SST 6.0 °C) than in the two previous AT surveys (7.1 °C in 2022 and 8.5°C in 2018). 2024 SSTs were similar to SSTs in previous cold years (2006-2012; mean SST between 4.9 and 6.8 °C). Bottom temperatures in 2024 were the same as in 2022 (2.3 °C) and cooler than in 2018 (3.7 °C).

CONTENTS

INTRODUCTION

Scientists from the Midwater Assessment and Conservation Engineering (MACE) Program of the Alaska Fisheries Science Center's (AFSC) Resource Assessment and Conservation Engineering (RACE) Division have conducted summer acoustic-trawl (AT) stock assessment surveys to estimate the abundance and distribution of walleye pollock on the Eastern Bering Sea (EBS) shelf since 1979. Surveys were conducted triennially through 1994 and have been conducted either annually or biennially since 1994. The surveys generally extend from seafloor depths of 50 m to 1,000 m, encompassing the middle (50 to 100 m isobaths) and outer (100 to 200 m isobaths) domains of the Bering Sea shelf.

The 2024 AT survey was carried out between 11 June and 18 July aboard the NOAA Ship *Oscar Dyson*. The primary objective was to collect acoustic and trawl information to estimate pollock midwater abundance and distribution within the U.S. portion of the Bering Sea shelf using AT survey methods.

Due to a delayed departure and uncertainty about survey completion caused by funding shortages and a shipboard COVID outbreak, the survey was conducted at a lower resolution (i.e., increased transect spacing, less trawling), and over a shorter time period, than in the past. This resulted in the traditional (core) area being surveyed over 2 legs/ 6 weeks versus the standard 3 legs/ 9 weeks. After the survey area was completed at 40 nmi transect spacing, there was sufficient time remaining to add transects on the northwestern shelf, resulting in 20-nmi spacing in this area. The impacts of surveying at 40 nmi versus 20 nmi transect spacing are explored in Appendix IV.

Although the Russian portion of the EBS shelf and the inshore areas north of St. Matthew Island have been surveyed intermittently in previous surveys, neither was surveyed in 2024. Additional sampling included conductivity-temperature-depth (CTD) probes to characterize shelf oceanographic conditions, and small-mesh midwater (Methot) trawls to characterize zooplankton backscatter in order to obtain an index of euphausiid (order Euphausiacea) abundance.

This report presents the 2024 pollock distribution and abundance estimates by size and age from near the sea surface to 0.5 m off the seafloor. Other survey results presented include 1) acoustic system calibration, 2) physical oceanographic (temperature) spatial patterns, 3) pollock biomass spatial patterns, 4) spatial patterns of non-pollock backscatter, 5) pollock vertical distributions, and 6) AT survey time series of pollock abundance estimates.

METHODS

All activities were conducted aboard the NOAA Ship *Oscar Dyson*, a 64-m stern trawler equipped for fisheries and oceanographic research. The survey followed established AT methods as specified in NOAA protocols for fisheries acoustics surveys and related sampling[1]. The acoustic units used here are defined in MacLennan et al. (2002). Survey itineraries are listed in Appendix I and scientific personnel in Appendix II.

Acoustic Equipment, Calibration, and Data Collection

Acoustic measurements were collected with a Simrad EK80 scientific echosounder (Bodholt and Solli 1992, Simrad 2018). Data were collected with five split-beam transducers (18, 38, 70, 120, and 200 kHz) mounted on the bottom of the vessel's retractable centerboard, which was extended 9.15 m below the water surface.

Two standard sphere acoustic system calibrations were conducted to measure acoustic system performance (Table 1). The vessel's dynamic positioning system was used to maintain the vessel location during calibration. Local water temperature and salinity were measured and used to estimate absorption and sound speed. A tungsten carbide sphere (38.1 mm diameter) suspended below the centerboard-mounted transducers was used to calibrate the five frequency systems. A two-stage calibration approach was followed for each frequency. On-axis sensitivity (i.e., transducer gain and S_a correction) was estimated from measurements with the sphere placed in the center of the beam following the procedure described in Foote et al. (1987). Transducer beam characteristics (i.e., beam angles and angle offsets) were estimated by moving the sphere in a horizontal plane using the EK80's calibration utility (Jech et al. 2005, Simrad 2018). The equivalent beam angle (for characterizing the volume sampled by the beam) and angle

[1] National Marine Fisheries Service (NMFS) 2014. NOAA protocols for fisheries acoustics surveys and related sampling (Alaska Fisheries Science Center), 26 p. Prepared by Midwater Assessment and Conservation Engineering Program, Alaska Fish. Sci. Center, Natl. Mar. Fish. Serv., NOAA.

sensitivities (for conversion of electrical to mechanical angles) cannot be estimated from the calibration approach used because that requires knowledge of the absolute position of the sphere (see Demer et al. 2015). Therefore, the factory default values for equivalent beam angle and angle sensitivities for each transducer were used during calibration.

Raw acoustic data were recorded using EK80 software (version 23.6.2) at a median ping interval of 1.3-1.4 seconds at water depths ≤ 400 m and 6 seconds or longer at water depths > 400 m, and analyzed from 16 m below the sea surface to within 0.5 m of the sounder-detected bottom to a maximum depth of 1,000 m. Data shallower than 16 m were excluded to account for the acoustic near-field range of all transducers (Simmonds and MacLennan 2005). Data within 0.5 m of the seafloor were also excluded to account for the bottom-associated acoustic dead zone (Ona and Mitson 1996). The raw acoustic data were analyzed using Echoview post-processing software (version 14.0.206, Echoview Software Pty Ltd).

Trawl Gear and Oceanographic Equipment

Midwater acoustic backscatter was sampled using an LFS1421 trawl[2]. The headrope and footrope of the LFS1421 trawl each measure 76.8 m (252 ft), with meshes tapering from 650 cm (256 in.) in the forward sections to 3.8 cm (1.5 in.) in the section immediately preceding the codend (mesh sizes are stretched measurements unless otherwise noted). To increase retention of small organisms, the LFS1421 codend was fitted with a knotless nylon 7.9 mm (5/16 in.) mesh, 3.2 mm (1/8 in.) square-opening codend liner.

The LFS1421 trawl was fished with four 45.7 m (150 ft) bridles (1.9 cm (0.75 in.) dia.), 5 m^2 Series-2000-V trawl doors with 4 in. shoes (918 kg (2,024 lb) each), and 227 kg (500 lb) tom weights attached to each wingtip. Average trawling speed was 1.6 m s^{-1} (3.2 knots). LFS1421 trawl vertical net openings and headrope depths were monitored with a Simrad FS70 third-wire netsonde attached to the headrope. The vertical net opening of the LFS1421 trawl ranged from 12.6 to 25.8 m (41.3 to 84.5 ft) and averaged 16.7 m (54.8 ft) while fishing. Near-bottom backscatter (between 3.0 m and 0.5 m off bottom) was sampled using 83-112 Eastern bottom trawls with a 25.3 m (83 ft) headrope and 34.1 m (112 ft) footrope and 3.5 in. codend mesh.

[2] LFS1421 trawl (LFS Marine, NOAA, 1421 Research Trawl, designed and built in 2018/2019 to MACE specifications; hereafter LFS1421)

Hauls were made on a regular 20 × 20 nmi grid during the 2024 EBS bottom trawl (BT) survey carried out between 30 May and 29 July (e.g., see Markowitz et al. 2023 for details.)

A Methot trawl (Methot 1986) was used to target midwater acoustic layers containing macro-zooplankton such as euphausiids, age-0 walleye pollock, and larval fishes. The Methot trawl had a rigid square frame measuring 2.3 m (7.5 ft) on each side, which formed the mouth of the net. The body of the net consisted of nylon 63.5 mm (2.5 in.) mesh material, lined with delta nylon 1/8 in. mesh material with 2 mm × 3 mm oval openings, and attached to a hard plastic codend bucket lined with 1 mm × 1 mm square opening mesh. A 1.8 m (5.9 ft) dihedral depressor was used to generate additional downward force. A calibrated General Oceanics flowmeter was attached to the mouth of the net; the number of flowmeter revolutions and the total time the net was in the water were used to determine the volume of water filtered during the haul. The Methot trawl was attached to a single cable fed through a stern-mounted A-frame. Real-time haul depths were monitored using a Simrad ITI acoustic link temperature-depth sensor attached to the bottom of the Methot frame. The Methot trawl was towed at an average speed of 1.3 m s^{-1} (2.6 knots).

To estimate escapement of smaller fishes from the net, recapture (or pocket) nets were placed at several locations along the LFS1421 net as was done during previous surveys (Williams et al. 2010, Honkalehto et al. 2022). The LFS1421 trawl was fitted with a total of nine recapture nets placed on forward (813 mm mesh), mid (102 mm mesh), and aft (102 mm mesh) sections of the trawl, with one recapture net attached on the top, bottom, and port panel of each section. The recapture nets were constructed from knotless nylon 7.9 mm (5/16 in.) mesh, 3.2 mm (1/8 in.) square-opening mesh material (matching the codend liner).

A stereo camera system (Camtrawl; Williams et al. 2010) was attached to the starboard panel forward of the codend on the LFS1421 trawl. The Camtrawl was used to capture stereo images for species identification and length measurement of individual fish and other taxa as they passed through the net toward the codend. The Camtrawl data were useful for determining the depth and size distribution of fish and other taxa when distinct and separate backscatter layers were sampled by a trawl haul but could not be differentiated in the codend catch. Images were viewed and annotated using procedures described in Williams et al. (2010).

Physical oceanographic data were collected during the cruise at trawl locations, at calibration locations, and continuously along transects. Water temperature profiles were obtained at trawl locations with a temperature-depth probe (SBE 39, Sea-Bird Scientific) attached to the trawl headrope. Additional temperature-depth measurements were taken from conductivity-temperature-depth (CTD) casts with a Sea-Bird CTD (SBE 911plus) system at the calibration site and throughout the survey to describe EBS shelf temperature features associated with pollock and euphausiids. A total of 40 CTD casts were made during the survey, including 24 made at or near the night break transect point, and 16 made at the closest point along a survey transect to 16 nominal stations, selected to provide a systematic, representative set of water column observations (P. Stabeno, PMEL, pers. commun.) to complement SBE profiles. This sampling strategy is repeatable each survey year with minimal impact on other survey operations. Salinity bottle samples (e.g., one bottle every other day, alternating at surface and bottom of cast) were collected from the casts to calibrate the CTD conductivity sensor. Sea surface temperature (SST) data were measured using the ship's SST system (SBE 38, Sea-Bird Scientific, accuracy ± 0.002°C) located near the ship's bow, approximately 1.4 m below the surface. At times when the SBE 38 was not operating, sea surface temperatures were taken from the Furuno T-2000 temperature probe (accuracy ± 0.2°C) located amidships 1.4 m below the surface. The SBE 38 was used 95.4% of the time and the Furuno was used 4.6% of the time in this survey. These and other environmental data were recorded using the ship's Scientific Computing Systems (SCS).

Survey Design

The 2024 survey design consisted of a series of parallel transects spaced 74 km (40 nmi) apart. Traditionally, this survey consists of parallel transects spaced 37 km (20 nmi) apart and is conducted over three ca. 3-week long legs. After the survey area was completed at 40 nmi transect resolution, transects were added on the northwestern shelf, resulting in a transect resolution of 20 nmi in this area.

Trawl hauls were conducted to identify the species and size composition of acoustically-observed fish aggregations and to determine biological characteristics of pollock and other specimens. Catches were sorted to species and weighed. When large numbers of juvenile and adult pollock were encountered, the predominant size groups in the catch were sampled separately (e.g., age-1 vs. larger sizes). Fork length (FL), body weight, sex (FL > 20 cm), maturity, age (otoliths), and gonad measurements were collected for a random subset of pollock within each size group. Pollock and other fishes were measured to the nearest 1 mm FL, or standard length (SL) for small specimens, with an electronic measuring board (Towler and Williams 2010). All lengths measured as SL were converted to FL using an SL to FL regression obtained from historic survey data when necessary. Other invertebrate organisms (e.g., jellyfish, squid) were measured to the nearest 1 mm length using accepted measurements for their class (e.g., jellyfish bell diameter, squid mantle length). Gonad maturity was determined by visual inspection and categorized as immature, developing, mature (hereafter, "pre-spawning"), spawning, or spent[3]. The ovary weight was determined for pre-spawning females. An electronic motion-compensating scale (Marel M60) was used to weigh individual pollock and selected ovaries to the nearest 2 g. Otoliths that were collected were stored in 50% glycerin/thymol/water solution and interpreted by AFSC Age and Growth Program researchers to determine fish ages. Trawl station information and biological measurements were electronically recorded using the MACE Program's custom Catch Logger for Acoustic Midwater Surveys (CLAMS) software.

The catch from Methot trawl hauls was transferred to a large tote. Large organisms (such as jellyfish) and small fishes were removed, identified, weighed, and measured. The remainder of the catch was placed on a 1 mm mesh screen to remove excess water and weighed. A subsample of the zooplankton mixture was then weighed and sorted into broad taxonomic groups for which a count and weight were determined. A second subsample was weighed and preserved in a 5% buffered formalin solution for more detailed enumeration at the Polish Sorting Center in Szczecin, Poland.

Additional biological samples were collected for special projects. Pollock ovaries were collected from pre-spawning walleye pollock to investigate interannual variation in fecundity of mature females (Sandi Neidetcher, Sandi.Neidetcher@noaa.gov), and from female walleye pollock of all maturity stages for a histological study. Chinook salmon (*Oncorhynchus tshawytscha*) heads were collected to contribute to a more comprehensive understanding of the distribution of Chinook salmon stocks in the North Pacific Rim (Kathrine Howard,

[3] 2024 Groundfish Survey Data Codes and Forms. 2024. RACE Division, AFSC, NMFS, NOAA; 7600 Sand Point Way NE, Seattle, WA 98115. DOI: https://doi.org/10.25923/gt9j-rs58.

kathrine.howard@noaa.gov). Whole specimens were collected from northern smoothtongue (*Leuroglossus schmidti*) to develop critical genetic primers for the northern fur seal prey sequence library (Katie Luxa, katie.luxa@noaa.gov).

Additionally, three moorings were deployed and retrieved during the survey. These moorings were used to track the timing and occurrence of marine mammal species in the Bering Sea and to monitor changes in their acoustic environment (Catherine Berchok, Catherine.Berchok@noaa.gov).

Data Analysis

Pollock abundance was estimated by combining acoustic and trawl catch information. The analysis method employed here had three principal steps. First, backscatter was associated with the trawl catches from the nearest geographic haul locations within a stratum. Second, a correction was made for net selectivity (escapement from the midwater net, based on relationships derived from recapture nets; Williams et al. 2011). Third, backscatter was converted to estimates of abundance using the nearest-haul catch association (step 1) with sample corrections (step 2) and the expected backscatter from each organism given species and size. Biomass was computed from abundance using the mean weight-at-length from all pollock specimens measured in the survey.

Processing of Acoustic Data

Although acoustic data were recorded at five frequencies, the results of this report and the survey time series are based on the 38 kHz data. The sounder-detected bottom was calculated by averaging the bottom detections for the five frequencies (Jones et al. 2011) and then visually examined to remove any bottom integrations. A minimum S_v threshold of –70 dB re 1 m^{-1} was applied to the 38 kHz acoustic data, which were then echo-integrated from 16 m below the surface to 0.5 m above the sounder-detected bottom. Data were averaged at 0.5 nmi horizontal by 10 m vertical resolution intervals and exported to a database.

Associating Size and Species Composition with Acoustic Backscatter

Acoustic backscatter was assigned to strata based on the appearance and vertical distribution of the aggregations in the echogram. Strata containing backscatter not considered to be from pollock (e.g., the near-surface mixture of unidentifiable backscatter, backscatter with frequency response indicative of euphausiids or myctophids (De Robertis et al. 2010), or near-bottom backscatter "haystack" morphology indicative of some rockfishes that could not be sampled) were excluded from further analyses. Each trawl was associated with a stratum, and the backscatter at a given location was associated with the species and size composition of the geographically-nearest haul within that stratum (see De Robertis et al. 2017b for details). For example, juvenile pollock can be found in shallow, dense schools with a diffuse layer of adult pollock at deeper depths in the same area. In this case, the backscatter dominated by aggregations of juveniles would be assigned to a shallow stratum (A) and the backscatter dominated by adult layers would be assigned to a deep stratum (B). Hauls that sampled the shallow layer would be assigned to stratum A, and hauls that sampled the deeper layer would be assigned to stratum B. Backscatter was apportioned by species and size within a stratum using the selectivity-corrected catch composition from the geographically nearest trawl in that stratum and converted to abundance.

Accounting for Catch from Non-Targeted Scattering Layers

As noted above, each trawl was associated with an acoustic stratum. However, trawls may capture animals while passing through non-targeted strata during the trawling process. For example, a trawl targeting a deep stratum may capture acoustically-relevant animals while passing through a shallower stratum during set and retrieval. Because trawls aggregate catch from all the strata sampled, animals from the shallow stratum could then be associated incorrectly with the deeper stratum during analysis. These animals should not be included in the catch that is applied to the deeper stratum.

To avoid incorrectly applying catch from different strata, Camtrawl images collected during LFS1421 trawls were used to identify catch depth and location in the water column. Camtrawl images were captured at a rate of approximately 1 s^{-1} and each image was tagged with collection time and depth. Analysts visually identified and counted animals present in every 100th image (approximately one image per 1.5 minute of trawl time) using SEBASTES Stereo Image Analysis software (Williams et al. 2016). For every examined image, the analyst identified all visible fish to the lowest taxonomic level possible, and identified invertebrates to broad taxonomic group (i.e., 'jellyfish,' 'squid,' 'shrimp'). Images were then examined using custom

Python applications to identify cases where the trawl retained catch from non-targeted layers. In rare, exceptional cases where it was evident that the trawl catch contained acoustically-relevant species and/or size classes from outside of the target stratum, these species and/or size class records were excluded during the analysis process from the trawl catch associated with the target stratum (see Figs. 3 and 4 in Levine et al. 2024 for a summary of the review process).

Selectivity Correction

Previous research has found that smaller pollock are less likely to be retained in large midwater trawls than larger pollock (Williams et al. 2011). To correct for species- and size-related differences in retention, trawl catch compositions were adjusted to that which would be expected from an unselective net. Trawl selectivity was estimated using correction functions developed from catch data collected by recapture nets mounted on the midwater trawl. Trawl selectivity in the 2024 survey was estimated for all species observed in the codend using correction functions developed from catch data collected by recapture nets mounted on the LFS1421 trawl during the 2022 summer EBS AT survey (Stienessen et al. 2025). No selectivity correction has been estimated for the bottom trawl. The counts and weights of fish and other taxa caught in the recapture nets were expanded to provide an estimate of escapement from the entire trawl. The catch of all species was corrected for the estimated probability of escapement by dividing the abundance of a given species and size class by the estimated probability of retention of that species and size class. The probability of retention was calculated using either species-specific trawl selectivity correction functions for the most abundant species or more generic selectivity functions for less abundant species that were pooled together (De Robertis et al. 2017b, Honkalehto et al. 2022). Thus, the 2024 survey estimates reflect adjustments to the trawl-derived estimates of species and size composition which incorporate the estimated escapement of all organisms from the catch (e.g., De Robertis et al. 2017a).

Abundance Calculations

A series of target strength (TS, dB re 1 m^2; the expected backscatter from each organism) to length relationships from the literature (Table 2) were used along with size and species distributions from selectivity-corrected trawl catches to estimate the proportion of the observed acoustic scattering attributable to each of the species captured in the trawls (Appendix III). For species for which the TS-length relationship was derived using a different length measurement type than the one used for measuring the trawl catch specimens, an appropriate length conversion was applied (e.g., total length to fork length). Species-specific TS-length relationships from the literature were used for pollock, Pacific capelin, eulachon, Pacific herring, and for any species whose contribution to the total backscatter used in survey estimates was > 5%. Otherwise, species were assigned to one of five group TS-length relationships: fishes with swim bladders, fishes without swim bladders, jellyfish, squid, and pelagic crustaceans (Table 2).

Due to geographic growth differences, walleye pollock are typically larger and heavier at age, east than west of 170° W (Traynor and Nelson 1985, Honkalehto et al. 2002). Therefore, biomass was computed from abundance using the mean weight-at-length from all pollock specimens lengthed and weighed in the survey trawl catches using two length-weight keys, one for east and one for west of 170° W (Appendix III). When < 5 pollock occurred within a 1-cm length interval, weight at a given length interval was estimated from a linear regression of the natural logs of the length and weight data and corrected for a small bias due to back-transformation (Appendix III; Miller 1984, De Robertis and Williams 2008).

Two age-length keys and a proportion-at-age matrix were applied to the population numbers-at-length and biomass-at-length to estimate numbers and biomass at age, one for east and one for west of 170° W (Appendix III; Jones et al. 2019). For population estimates at lengths where no otolith specimens were collected, the proportion-at-age was estimated using a Gaussian-model approach based on historical age-at-length data (1999-2016).

Processing of Maturity Data

Maturity data by haul were weighted by the local acoustically-estimated abundance of adult pollock (number of individuals > 30 cm FL). The 30 cm size criterion was selected as the approximate minimum size at which ≥ 5% of pollock are mature. The sum of the local abundance, A_h, assigned to the geographically-nearest haul was computed. A weight, W_h, was then assigned to each haul by dividing the local abundance A_h by the average abundance per haul $\overline{A}$:

$$W_h = \frac{A_h}{\overline{A}} \quad , \qquad \text{(Eq. 1)}$$

where

$$\overline{A} = \frac{\sum_h A_h}{H} \qquad \text{(Eq. 2)}$$

and H is the total number of hauls.

The percent of pollock, $PP_{sex,mat}$ > 40 cm by sex and maturity stage (immature, developing, pre-spawning, spawning, or spent) was computed for each haul and combined by survey area using a weighted average with W_h:

$$PP_{sex,mat} = \frac{\sum_h \left(N_{sex,mat,h} \cdot W_h\right)}{\sum_h W_h} , \qquad \text{(Eq. 3)}$$

where $N_{(sex,mat,h)}$ is the number of pollock > 40 cm by sex and maturity for each haul. The > 40 cm cutoff was used for consistency with reporting from past surveys.

Near-bottom Analysis

Historically, AT survey results on the U.S. EBS shelf (i.e. "core area") were presented for the water column between 16.0 m and 3.0 m off the seafloor. The analysis did not extend deeper than 3.0 m above the seafloor because 1) diverse catches in bottom trawl survey suggested that pollock may not dominate the backscatter close to the seafloor, and 2) the annual bottom trawl (BT) survey samples to a nominal depth of 2.5-3.0 m above the seafloor in the U.S. Exclusive Economic Zone (EEZ; Markowitz et al. 2023). An approach was developed (Lauffenburger et al. 2017) to estimate the acoustic contribution of pollock relative to other species in the diverse region between 0.5 and 3.0 m off bottom. This approach uses backscatter data from the AT survey scaled with catch data in this region from the summer BT survey conducted in the same year, first applied to EBS survey results in 2016 (Honkalehto et al. 2018, Stienessen et al. 2025).

Relative Estimation Error

Transects were parallel and relative estimation errors for the acoustic-based estimates were derived using a one-dimensional (1-D) geostatistical method (Petitgas 1993, Williamson and Traynor 1996, Walline 2007). Relative estimation error is defined as the ratio of the square root of the 1-D estimation variance ($variance_{sum}$) to the biomass estimate (i.e., the sum of biomass over all transects, $biomass_{sum}$, kg):

$$Relative\ estimation\ error_{1-D} = \frac{\sqrt{variance_{sum}}}{biomass_{sum}} . \qquad \text{(Eq. 4)}$$

Because sampling resolution affects the variance estimate, and the 1-D method assumes equal transect spacing, estimation variance was determined separately in each area with unique transect spacing. Relative estimation error for an entire survey area (among n survey areas with different transect spacings) was computed by summing the estimation variance for each area j, taking the square root, and then dividing by the sum of the biomass over all areas, assuming independence among estimation errors for each survey area (Rivoirard et al. 2000):

$$Relative\ estimation\ error_{1-D\ survey} = \frac{\sqrt{\sum_{j=1}^{n} variance_{sum_j}}}{\sum_{j=1}^{n} biomass_{sum_j}} . \qquad \text{(Eq. 5)}$$

Geostatistical methods were used to compute estimation error to account for estimation uncertainty arising from the observed spatial structure in the fish distribution. These errors, however, quantify only across-transect sampling variability of the acoustic data (Rivoirard et al. 2000). Other sources of error (e.g., target strength, trawl sampling) were not evaluated.

Additional Analyses

Pollock vertical distribution patterns were examined using two metrics: 1) mean weighted depth (MWD) of pollock from the surface-referenced primary analysis, and 2) height above bottom (HAB), also calculated from the primary analysis, in which pollock vertical position was calculated as distance above the seafloor. The MWD in each along-track interval i is computed as:

$$MWD_i = \sum_j \left(\left(\frac{B_{i,j}}{\sum_j B_{i,j}} \right) d_{i,j} \right) , \qquad \text{(Eq. 6)}$$

where $B_{i,j}$ is observed biomass in 0.5 nmi along-track interval i and 10 m depth bin j, and d is the depth in meters of bin i from the sea surface. The HAB is computed in a similar fashion:

$$HAB_i = \sum_j \left(\left(\frac{B_{i,j}}{\sum_j B_{i,j}} \right) h_{i,j} \right) , \qquad \text{(Eq. 7)}$$

where the terms are as described above and h is the height in meters of bin i above the sounder-detected bottom. MWD and HAB were summarized for a given survey area by first summing biomass over all intervals i in the area and then computing the MWD and HAB using the equations above.

RESULTS AND DISCUSSION

Acoustic System Calibration

Pre- and post-survey calibration measurements of the 38 kHz echosounder, made on 7 June and 19 July, showed no notable differences in on-axis gain parameters or beam pattern characteristics confirming that the acoustic system was stable throughout the survey (Table 1). The on-axis results were used to calculate gain, while the swing results were used to verify that the beam pattern matched expectations. Acoustic system gain and beam pattern parameters measured during the first and second calibrations were averaged (averages calculated in the linear domain for dB quantities), nominal sound speed and absorption values appropriate for the survey areas were used in the final parameter set for survey data analysis, and the equivalent beam angle initially measured by the manufacturer in a test tank was adjusted (Bodholt 2002) using the in-situ sound speed during survey conditions (Table 1).

Survey Timing and Extent

The Bering Sea summer AT survey was conducted between 11 June and 18 July. The entire survey area encompassed 349,113 km^2 (101,785 nmi^2). Acoustic backscatter was measured along 6,203.1 km (3,349.4 nmi) of trackline on 18 transects spaced from 37.0 km (20.0 nmi) to 74.1 km (40.0 nmi) apart, depending on the survey region (Fig. 1). Surveyed bottom depths ranged from 32 to 1,000 m and averaged 141 m.

Water Temperature

The mean SST during the 2024 survey was 6.0°C (range 2.6°-8.2°C; Fig. 2a). The mean bottom temperature, as measured during 40 CTD deployments during 2024, was 2.3°C (range -1.3°C -

5.0°C; Fig. 2b). Sea surface temperatures (SST) were cooler in 2024 than in the two previous AT surveys (7.1°C in 2022 and 8.5°C in 2018). They were similar to SSTs in previous cold years (2006-2012; mean SST between 4.9°C and 6.8°C). The warmest SSTs observed in the 2024 EBS survey were on the south end of transect 21, west of the Pribilof Islands and south of Zhemchug Canyon (mean 7.6°C, max 8.2°C). Transect 21 was the last transect surveyed in mid-July as the ship returned to port. SSTs were coolest between the Pribilof Islands and St. Matthew Island in mid-to-late June. Bottom temperatures in 2024 were the same as in 2022 (2.3°C) and cooler than in 2018 (3.7°C), and characteristic of the 'cold pool' (< 2.0°C; Wyllie-Echeverria and Wooster 1998), which is mainly driven by the extent of sea ice in the prior winter.

Temperature-depth profiles from trawl headrope sensors indicate that the water column was vertically stratified with a thermocline at roughly 15-25 m from the surface (Fig. 3). The EBS shelf region west of 170°W was more vertically stratified (4°C cooler below the thermocline, Fig. 3) than east of 170°W. Trawl headrope temperatures below the thermocline were warmer on average east of 170°W (> 4°C) than west of 170°W (≥ 2°C).

Trawl Sampling

Biological data and specimens applied to the midwater backscatter observed between the near-surface and 3.0 m off bottom were collected from 55 LFS1421 and 3 Methot deployments, of which 54 LFS1421 hauls were used in fish abundance estimate calculations (Fig. 1, Table 3). In cases where hauls were excluded from fish abundance calculations, this was due to low catch and/or mechanical issues during the trawl. Pollock and Chrysaora jellyfish were the most abundant species by weight in LFS1421 trawls, contributing 88.6% and 11.0% of the catch by weight (Table 4). Pollock and chrysaora jellyfish were the most abundant species by number in the LFS1421 trawls, contributing 95.6% and 3.5% of the catch by number (Table 4). Chrysaora jellyfish and euphausiids were the most abundant species by weight in Methot trawls, contributing 86.7% and 11.1% of the catch by weight (Table 5). Euphausiids and chrysaora jellyfish were the most abundant species by number in the Methot trawls, contributing 99.5% and 0.5% of the catch by number (Table 5). Although catch composition from the Methot trawls is reported here, the survey abundance and biomass estimates of euphausiids, derived in part from the Methot catch data, are reported elsewhere (Levine and Ressler 2024). Biological data and specimens applied to the near-bottom backscatter (0.5 m off bottom - 3.0 m off bottom) were from 350 BT survey 83-112 hauls conducted in the core area (Markowitz et al. 2023).

Pollock Weight, Length, Maturity, and Age

Length was measured from 19,007 age 1+ pollock, and weight and length were measured from 3,501 pollock during the 2024 EBS summer survey (Table 6). For non-pollock species and age-0 pollock, lengths were measured from 1,516 specimens, and 918 weights were collected. Pollock weight at length during the 2024 EBS survey was lighter than that in previous surveys (Fig. 4).

Almost all male and female adult pollock sampled for maturity throughout the survey were in the developing or spent stages of maturity (91% and 93%, respectively; Fig. 5). There is some ambiguity as to exactly when the stage of maturity reverts from spent back to developing prior to active spawning again. Less than 1% of pollock sampled were actively spawning.

Otoliths were collected from 2,286 pollock (Table 6), of which 2,260 were aged and used to scale acoustic backscatter. Mean length and weight at age of pollock for 2024 were plotted against comparable mean data from combined AT surveys between 2004 and 2022 (Fig. 6). Younger fish (≤ age-5) east of 170°W were longer and heavier when compared to the same aged fish found west of 170°W, which supports the use of two length-weight keys (Fig. 6).

Pollock Distribution

About 68% of the total acoustic backscatter observed between 16.0 m below the surface and 3.0 m off bottom (the midwater layer) during the 2024 survey was attributed to pollock. This was a higher fraction of pollock backscatter than that observed in AT surveys between 2012 and 2022 (range 35 - 56%), and much less than that observed in 2010 (82%; Honkalehto et al. 2012, 2013, 2018, Honkalehto and McCarthy 2015, McCarthy et al. 2020, Stienessen et al. 2025). Pollock in 2024 were observed in a variety of aggregations including near-bottom layers, small dense schools (cherry balls) in midwater, and diffuse aggregations of individual fish. The remaining non-pollock midwater backscatter was attributed to an undifferentiated plankton-fishes mixture (27%), or in a few isolated areas, to myctophids and other fishes (3%). The near-bottom analysis (0.5-3.0 m above the seafloor) attributed ~92% of the backscatter in that zone to pollock.

Pollock were observed throughout the survey area. Locally dense pollock aggregations were observed between the 100 m contour and the shelf break, particularly north of Unimak Pass in the Bering Canyon and between Zhemchug Canyon and the U.S.-Russia Convention line (Fig. 7).

Pollock Abundance and Biomass

The estimated abundance of pollock in midwater (between 16.0 m from the sea surface and 0.5 m off the seafloor) in the core survey area was 11.4 billion fish weighing 2.9 million metric tons (t) (Tables 7-11, Fig. 8). This represents a 17.4% increase in numbers of fish and a 25.0% decrease in biomass from the 2022 summer EBS survey (Fig. 8). The 2024 abundance estimates are 4.4% above (by numbers) and 20.9% below (by weight) the 2012-2022 mean abundance estimates for the core survey regions that have been consistently sampled since 2012. The relative estimation error of the overall biomass based on the 1-D geostatistical analysis was 5.6% (Table 9). Despite the increase in transect spacing from 20 nmi to 40 nmi over the EBS shelf, the estimation error remained similar to those from prior 20-nmi spaced surveys (range 1.9-6.9%).

Pollock biomass west of 170° W made up 62% of the total estimated survey biomass and 46% of the total abundance (Table 9). In 2022, the area west of 170°W had 64% of the core area biomass; in 2020 it had 74% of the biomass, and in 2018, 70% (Table 9). East of 170°W, the 2024 biomass was 0.6 million t, 21% of the total EBS biomass. This was a small decline from 2022 (0.9 million t; 22% of the core biomass), and an increase over 2020 (0.5 million tons; 15% of the core biomass). Pollock biomass increased inside the Steller sea lion Conservation Area (SCA) from 0.40 million t in 2020, to 0.54 million t in 2022, and decreased slightly in 2024 to 0.5 million t (Table 9). The pollock biomass within the SCA in 2024 was close to the mean of the last 5 survey years (2014-2022, 0.46 million tons), and three times the mean biomass from 2004-2012 (0.18 million tons).

Pollock Length, Weight, and Age Composition

Age-1+ pollock ranged in length from 9 to 77 cm FL with modes at 13 and 42 cm FL (Fig. 9; Tables 7 and 8). Approximately 44% of total pollock numbers were attributed to age-1 fish from the 2023 year class, with age-6 and age-5 pollock from the 2018 and 2019 year classes (the second and third most abundant age classes by number) contributing 22% and 9%, respectively, of total abundance (Figs. 10 and 11a; Table 10). Approximately 48% of total pollock biomass was attributed to age-6 fish from the 2018 year class, with age-5 and age-7 pollock from the 2019 and 2017 year classes (the second and third most abundant age classes by biomass) contributing 18% and 9%, respectively, of total pollock biomass (Figs. 10 and 11b; Table 11).

The age composition of pollock in the 2024 EBS summer survey was more broadly distributed across year classes for numbers and biomass than had been observed since 2014, especially in the area west of 170°W, primarily due to contributions from the 2017, 2018, and 2019 year classes (Figs. 11a and b). In contrast, in EBS surveys conducted from 2014 to 2018, the 2012 year class accounted for most of the observed pollock numbers and biomass. Age-1 and age-2 fish composed 6% of the core survey area biomass, and 54% of the core numbers, more than observed in any EBS survey since 2007 (Figs. 10, 11).

Pollock Vertical Distribution

The vertical distribution of pollock ≥ 30 cm FL in the core survey area exhibited clear differences between east and west of 170°W in the summer 2024 survey (Fig. 12). The estimated MWD for adult pollock east of 170°W was 68 m, and the estimated MWD for pollock west of 170°W was 84 m. In 2022, adult pollock were found deeper east of 170°W (95 m) than during the 2024 survey, and the difference in MWD between east and west (MWD west of 170°W: 86 m) was much smaller. Juvenile pollock (< 30 cm FL) in 2024 were found at 50 m MWD east of 170°W, and at 75 m MWD west of 170°W. Not enough juvenile pollock were seen in 2022 to allow calculations of MWD. Adult pollock east of 170°W were found closer to the seafloor than they were to the west of 170°W (Fig. 12). More than 73% of adult pollock east of 170°W were found within 50 m of the bottom, whereas 66% of the adult pollock west of 170°W were found within 50 m of the bottom. For juvenile pollock east of 170°W, more than 18% of the biomass was found within 50 m of the bottom, whereas 56% of the juvenile pollock west of 170°W were found within 50 m of the bottom.

Historical Population Trends

Spatial distributions of pollock biomass were evaluated in the EBS from 1994 to 2024, for those years in which the AT survey was conducted (Fig. 13). Pollock spatial distribution trends in midwater showed that overall biomass was relatively low from 2007 to 2012, and the majority of pollock biomass was concentrated west of 170°W during this period (Fig. 13). In 2014 and 2016, the proportion of pollock biomass increased in the southeast portion of the core area, resulting in a more widely distributed pollock spatial pattern. After 2016, the proportion of pollock biomass decreased in the southeast, but not to the low levels observed prior to 2014 (Fig. 13; Table 9). The highest pollock backscatter observed in 2024 was distributed at the head of Pribilof Canyon (~165° W) and west of St. Matthew Island in the center of the outer domain (Fig. 7).

Temporal patterns in pollock numbers and biomass-at-length and biomass-at-age were examined between 0.5 m off-bottom and near-surface. The 2012 year class (age-6 pollock in 2018, the second most abundant juvenile year class in the time series since 1994; Fig. 11, Table 10) and the 2013 year class (age-5 pollock in 2018), grew to dominate the midwater abundance between 2014 and 2018 in the Bering Sea (Figs. 11 and 14; Tables 10 and 11). By 2024, the presence of these two cohorts had declined as the fish aged, as expected. Their combined contribution was only 1.2% and 0.3% to the 2024 midwater pollock abundance by biomass and numbers, respectively, as age-12 and age-11 fish. Age-6 fish (length 34-60 cm) replaced them as the most dominant cohort in terms of biomass in 2024, contributing 47.7% and 22.2% to the midwater pollock biomass and numbers, respectively (Figs. 9 and 10; Tables 7-11).

The EBS pollock population tends to depend on the success of strong year classes at roughly a 3-5 year frequency (Ianelli et al. 2017). Years with good age-1 recruitment are evident in AT survey results (e.g., 1997, 2007-2010, and 2014) by the presence of relatively large numbers of 1-2 year-olds (Table 10; Fig. 11). The 2024 survey saw a large number of 1-2 year olds, similar to the strong age-1 years mentioned previously (Fig. 11). In 2022, Stienessen et al. (2025) noted that the dominant presence of the 2018 cohort suggested that the next strong year class would emerge sometime between 2021 and 2024, and the presence of age-2 (9.1% by numbers) and age-1 fish (44.5% by numbers) across the survey area support that suggestion. Age-1 fish in 2024 appear to be a strong year class.

Spatial distributions of non-pollock backscatter observed at 38 kHz were also evaluated in the EBS from 2007 to 2024, for those years in which the AT survey was conducted. Non-pollock backscatter is assumed to represent a temporally-varying mixture of largely unidentified zooplankton and fishes, sometimes including age-0 pollock. This backscatter has varied spatially over the AT survey time series. Most non-pollock backscatter has been observed in the upper part of the water column above the thermocline (Honkalehto and McCarthy 2015). Non-pollock backscatter observed in 2024 consisted of three connected patches: one on the west side of Bristol Bay, extending east-west across the shelf; the second on the mid-shelf to the northwest of the Pribilof Islands; and the third west of St. Matthew Island, in the northwest portion of the survey area (Fig. 15). Non-pollock backscatter observed in 2004 covered large portions of the survey area on the middle shelf from the Alaska Peninsula to Cape Navarin, Russia (see Honkalehto et al., 2018, Fig. 15). It diminished during years of relatively cold Bering Sea conditions between 2006 and 2010 and has been more widespread in recent years (Fig. 15). Concentrations were observed near the Pribilof Islands in most years since 2007, 2009-2010 being the exception. This backscatter information should be interpreted with caution because the biological composition of the scatterers is unknown.

Table 1. -- Simrad EK80 38 kHz acoustic system description and settings used during the summer 2024 Eastern Bering Sea acoustic-trawl survey. These include environmental parameters and results from standard sphere acoustic system calibrations conducted in association with the survey and final values used to calculate biomass and abundance data. The collection settings column contains 7 June EK80 calibration utility results. Other columns are a combination of on-axis and EK80 calibration utility results (see Methods and Results and Discussion sections of text for details).

	Survey collection settings	7 June Kalsin Bay Kodiak	19 July Makushin Bay Unalaska	Final analysis settings
Echosounder	Simrad EK80	Simrad EK80	Simrad EK80	Simrad EK80
Transducer	ES38-7 s/n 324	ES38-7 s/n 324	ES38-7 s/n 324	ES38-7 s/n 324
Frequency (kHz)	38.00	38.00	38.00	38.00
Transducer depth (m)	9.15	9.15	9.15	9.15
Pulse length (ms)	0.512	0.512	0.512	0.512
Transmitted power (W)	400	400	400	400
Angle sensitivity along	18.00	18.00	18.00	18.00
Angle sensitivity athwart	18.00	18.00	18.00	18.00
2-way beam angle (dB re 1 steradian)	-20.70	-20.70	-20.70	-20.50
Gain (dB)	27.12	24.04	27.04	27.04
S_a correction (dB)	-0.16	-0.14	-0.14	-0.14
Integration gain (dB)	26.96	26.90	26.90	26.90
3 dB beamwidth along	6.61	6.62	6.64	6.63
3 dB beamwidth athwart	6.65	6.65	6.68	6.67
Angle offset along	-0.05	-0.05	-0.05	-0.05
Angle offset athwart	0.07	0.07	0.07	0.07
Post-processing S_v threshold (dB re 1 m^{-1})	-70.00	--	--	-70.00
Standard sphere TS (dB re 1 m^2)	--	-42.45	-42.33	--
Sphere range from transducer (m)	--	20.61	19.86	--
Absorption coefficient (dB m^{-1})	0.009978	0.009701	0.009811	0.009978
Sound velocity (m s^{-1})	1470.0	1472.7	1474.0	1470.0
Water temp at transducer (°C)	--	6.41	7.09	--

Note: Gain and beam pattern terms are defined in the Operator Manual for Simrad EK80 Scientific echosounder application, which is available from Simrad Strandpromenaden 50, Box 111, N-3191 Horten, Norway.
-- symbol indicates the value is not applicable for the noted survey collection or calibration setting.

Table 2. -- Target strength (TS) to size relationships from the literature used to allocate 38 kHz acoustic backscatter to most species in this report. The symbols in the equations are as follows: r is the bell radius in cm and L is length in cm for all groups shown.

Group	TS (dB re 1 m^2)	Length type	TS derived for which species	Reference
pollock	$TS = 20 \log_{10} L - 66$	L = fork length	*Gadus chalcogrammus*	Foote and Traynor (1988), Traynor (1996)
Pacific capelin	$TS = 20 \log_{10} L - 70.3$	L = total length	*Mallotus catervarius*	Guttormsen and Wilson (2009)
Pacific herring[1]	$TS = 20 \log_{10} L - 2.3 \log_{10}(1 + depth/10) - 65.4$	L = fork length	*Clupea harengus*	Ona (2003)
eulachon	$TS = 20 \log_{10} L - 84.5$	L = total length	*Thaleichthys pacificus*	Gauthier and Horne (2004)
fish with swim bladders	$TS = 20 \log_{10} L - 67.4$	L = total length	Physoclist fishes	Foote (1987)
fish without swim bladders	$TS = 20 \log_{10} L - 83.2$	L = total length	*Pleurogrammus monopterygius*	Gauthier and Horne (2004)
jellyfish	$TS = 10 \log_{10}(\pi r^2) - 86.8$	r = bell radius	*Chrysaora melanaster*	De Robertis and Taylor (2014)
squid	$TS = 20 \log_{10} L - 75.4$	L = mantle length	*Todarodes pacificus*	Kang et al. (2005)
pelagic crustaceans[2]	$TS = A * (\log_{10}(BkL)/(BkL))^c + D((kL)^6) + E((kL)^5) + F((kL)^4) + G((kL)^3) + H((kL)^2) + I(kL) + J + 20 \log_{10}(L/L_0)$	L = total length	*Euphausia superba*	Demer and Conti (2005)

[1]*depth* (m) is fixed at 75 m.

[2]A = -930.429983; B = 3.21027896; C = 1.74003785; D = $1.36133896 \times 10^{-8}$; E = $-2.26958555 \times 10^{-6}$
F= $1.50291244 \times 10^{-4}$; G = $-4.86306872 \times 10^{-3}$; H = 0.0738748423; I = -0.408004891; J = -73.9078690; and L_0 = 0.03835
If L < 0.015 m, TS = -105 dB; and if L > 0.065 m, TS = -73 dB.
k = 2πfc, where f = 38,000 (frequency in Hz) and c = 1470 (sound speed in m s^{-1}).

Table 3. -- Trawl stations and catch data summary from the summer 2024 Eastern Bering Sea acoustic-trawl survey East and West of 170°W, and in the Steller sea lion Conservation Area (SCA).

Haul	Area	Gear	Date	Time	Duration	Start Position		Depth (m)		Temp (°C)		pollock		Other
No.		Type[a]	(GMT)	(GMT)	(mins)	Lat. (N)	Long. (W)	Headrope[b]	Bottom	Headrope	Surface[c]	(kg)	Number	(kg)
1	East of 170	LFS1421	12-Jun	05:42	40.5	56.0286	-162.7971	48	79	3.5	5.7	579.6	823	125.2
2	SCA	LFS1421	12-Jun	23:00	7.9	55.3353	-163.9883	53	75	4.4	5.8	169.4	333	440.1
3	East of 170	LFS1421	13-Jun	23:42	20.2	56.6063	-165.1912	41	78	4.0	5.3	602.0	2,060	155.1
4	SCA	LFS1421	14-Jun	05:51	24.7	55.8558	-165.1634	66	98	3.9	6.2	758.0	1,823	13.6
5	SCA	LFS1421	14-Jun	16:15	18.9	55.6392	-165.1589	27	109	4.7	6.1	327.0	17,327	33.4
6	SCA	LFS1421	14-Jun	23:20	17.3	54.9249	-165.1436	88	109	4.6	5.8	3,959.5	5,953	40.5
7	SCA	LFS1421	15-Jun	23:22	4.7	55.4995	-166.3453	83	129	4.2	6.5	568.5	31,693	9.4
8	East of 170	LFS1421	16-Jun	17:22	31.5	56.4822	-166.4010	34	98	3.7	6.0	196.3	347	301.2
9	East of 170	Methot	17-Jun	06:27	33.9	57.8950	-167.7564	-	68	-	4.2	-	-	32.5
10	East of 170	LFS1421	17-Jun	16:47	41.7	57.3766	-167.7077	46	73	2.5	4.9	830.4	1,375	159.2
11	East of 170	LFS1421	17-Jun	22:45	24.5	56.7008	-167.6446	70	96	3.5	6.8	342.5	721	52.0
12	East of 170	LFS1421	18-Jun	06:03	22.5	55.7789	-167.5627	96	135	4.0	6.4	115.3	1,926	6.5
13	East of 170	LFS1421	19-Jun	17:16	28.0	56.3154	-168.8300	97	125	4.0	6.8	780.3	1,318	3.2
14	East of 170	LFS1421	19-Jun	22:29	16.1	56.9011	-168.8972	55	83	3.0	7.0	615.6	1,597	49.3
15	East of 170	LFS1421	20-Jun	08:05	60.5	58.2669	-169.0614	43	70	1.8	6.2	461.0	751	61.5
16	West of 170	Methot	21-Jun	16:34	28.4	59.7377	-170.5771	46	67	-	6.2	-	-	6.0
17	West of 170	LFS1421	21-Jun	23:18	64.2	58.7633	-170.4199	40	73	0.7	5.7	271.4	423	33.5
18	West of 170	LFS1421	22-Jun	08:00	59.6	57.7549	-170.2591	35	75	0.7	6.1	324.2	599	78.5
19	West of 170	LFS1421	22-Jun	20:34	18.1	56.8198	-170.1156	46	83	3.1	6.7	1,119.5	2,125	312.0
20	West of 170	LFS1421	23-Jun	03:11	9.2	56.4277	-170.0543	88	107	3.3	7.1	377.3	663	19.5
21	West of 170	LFS1421	23-Jun	08:04	39.6	56.0781	-170.0035	73	126	3.6	6.7	228.7	326	0.7
22	West of 170	LFS1421	23-Jun	17:25	16.7	56.6071	-171.3037	91	123	3.3	6.9	509.5	843	53.4
23	West of 170	LFS1421	24-Jun	00:17	16.6	57.4970	-171.4629	73	100	1.8	7.6	453.9	873	361.5
24	West of 170	LFS1421	24-Jun	05:39	37.1	58.0924	-171.5712	70	99	1.2	6.8	375.7	887	139.7
25	West of 170	LFS1421	3-Jul	04:55	43.2	58.9568	-173.0249	67	109	1.6	5.6	906.2	2,105	215.0
26	West of 170	LFS1421	3-Jul	16:43	18.7	58.5178	-172.9352	70	111	1.5	5.8	685.7	6,250	463.9
27	West of 170	LFS1421	3-Jul	23:34	17.4	57.9678	-172.7997	77	110	2.2	6.2	769.7	1,899	282.6
29	West of 170	LFS1421	4-Jul	08:18	55.5	57.4752	-172.7057	70	120	2.5	6.3	220.9	434	9.2
30	West of 170	LFS1421	4-Jul	22:12	25.6	56.5777	-172.5245	182	208	3.8	6.5	10.5	17	11.5
31	West of 170	LFS1421	5-Jul	18:10	18.7	58.1380	-174.1172	80	140	3.2	6.6	564.3	1,153	57.9
32	West of 170	LFS1421	5-Jul	23:06	23.1	58.4669	-174.2035	99	135	2.8	6.1	616.6	1,176	81.7
33	West of 170	LFS1421	6-Jul	03:04	10.1	58.7799	-174.2660	80	139	2.5	6.0	2,118.2	4,287	126.7
34	West of 170	LFS1421	6-Jul	08:35	27.5	59.2381	-174.3993	71	122	1.9	5.9	481.1	1,149	175.8
35	West of 170	LFS1421	6-Jul	19:08	11.7	59.7633	-174.5246	80	115	1.5	5.7	756.9	4,333	61.4
36	West of 170	LFS1421	7-Jul	20:13	45.0	60.9813	-176.2629	81	114	1.2	5.2	665.4	2,411	45.3
37	West of 170	LFS1421	8-Jul	05:10	33.2	59.9775	-175.9472	83	131	1.8	-	587.9	1,320	15.5
38	West of 170	LFS1421	8-Jul	18:13	0.9	59.2862	-175.7347	56	138	2.8	6.6	550.5	3,616	53.3
39	West of 170	LFS1421	8-Jul	23:29	9.4	58.8530	-175.6039	80	131	2.1	6.8	692.2	1,423	13.5
40	West of 170	StereoDropCam	9-Jul	01:02	20.2	58.8642	-175.6185	-	-	-	-	-	-	-
41	West of 170	LFS1421	9-Jul	05:08	15.2	58.3966	-175.4685	-	216	-	6.5	881.8	1,575	10.7
43	West of 170	LFS1421	9-Jul	21:03	16.0	59.4945	-177.1035	98	150	2.1	6.3	586.6	1,151	22.5
44	West of 170	LFS1421	10-Jul	03:58	6.0	60.4038	-177.4049	121	153	1.1	6.3	982.8	10,134	20.6
45	West of 170	LFS1421	10-Jul	08:27	42.8	60.8627	-177.5908	97	139	0.9	6.3	895.5	8,607	34.5
46	West of 170	LFS1421	11-Jul	01:02	15.4	59.9521	-178.6041	80	140	2.2	7.2	235.5	484	15.7

Haul No.	Area	Gear Type[a]	Date (GMT)	Time (GMT)	Duration (mins)	Start Position Lat. (N)	Start Position Long. (W)	Depth (m) Headrope[b]	Depth (m) Bottom	Temp (°C) Headrope	Temp (°C) Surface[c]	pollock (kg)	pollock Number	Other (kg)
47	West of 170	LFS1421	11-Jul	22:39	22.3	59.7195	-177.8278	103	158	2.3	6.2	131.3	312	22.6
48	West of 170	LFS1421	12-Jul	02:52	10.8	60.0555	-177.9536	94	144	2.0	6.2	91.5	396	22.0
50	West of 170	LFS1421	12-Jul	09:22	52.6	60.5411	-178.1526	60	163	3.5	6.2	997.8	10,856	37.7
51	West of 170	LFS1421	13-Jul	05:09	22.5	60.2138	-176.6812	115	139	0.9	6.5	1,149.7	3,629	27.2
52	West of 170	LFS1421	13-Jul	18:14	24.8	59.2828	-176.3651	68	138	1.7	6.4	1,235.5	2,877	18.4
53	West of 170	LFS1421	14-Jul	08:25	18.5	58.9329	-174.9632	105	132	2.5	6.7	825.2	1,714	69.1
54	West of 170	LFS1421	14-Jul	19:07	28.0	59.5253	-175.1337	92	132	2.3	6.7	1,353.8	2,962	42.6
55	West of 170	LFS1421	15-Jul	03:01	43.3	60.5410	-175.4342	84	110	1.4	6.4	1,073.7	3,465	52.2
56	West of 170	Methot	15-Jul	17:29	60.1	61.5257	-175.7283	78	97	-	5.7	-	-	3.5
57	West of 170	LFS1421	16-Jul	03:05	51.2	60.4827	-174.0466	66	88	1.0	6.8	1,866.7	3,762	103.7
58	West of 170	LFS1421	16-Jul	16:16	34.0	59.7120	-173.8481	79	104	1.4	7.1	270.6	1,444	70.0
59	West of 170	LFS1421	17-Jul	00:17	17.6	58.8331	-173.6438	96	123	2.2	7.2	1,226.2	2,774	21.9
60	West of 170	LFS1421	17-Jul	05:05	15.0	58.3719	-173.5353	94	118	2.4	7.4	1,313.8	2,847	212.1
61	West of 170	LFS1421	17-Jul	16:46	9.2	57.9590	-173.4400	87	118	2.7	7.7	972.4	1,659	229.4
62	West of 170	StereoDropCam	17-Jul	18:51	21.3	57.9590	-173.4391	-	-	-	-	-	-	-
63	West of 170	StereoDropCam	17-Jul	20:22	20.6	57.9696	-173.4422	-	-	-	-	-	-	-
64	West of 170	StereoDropCam	17-Jul	21:19	21.0	57.9768	-173.4441	-	-	-	-	-	-	-
65	West of 170	LFS1421	18-Jul	07:11	24.1	56.7270	-173.1587	115	138	3.6	8.2	93.4	107	10.7

[a]LFS1421 = LFS1421 midwater trawl, Methot = Methot plankton net, StereoDropCam = camera drop on untrawlable areas.

[b]Headrope depth obtained from temperature-depth probe. In hauls without temperature-depth probe records, depth was obtained from scientist notes when possible.

[c]Average temperature measured from a temperature-depth probe (SBE 39, Sea-Bird Scientific).

Table 4. -- Catch by species and numbers of length and weight measurements taken from 55 LFS1421 hauls during the 2024 acoustic-trawl survey of the Eastern Bering Sea.

		Catch				Measurements	
Species name	Scientific name	Weight (kg)	%	Number	%	Length	Weight
pollock	*Gadus chalcogrammus*	39,775.6	88.6	167,114	95.6	19,007	3,501
chrysaora jellyfish	*Chrysaora* sp.	4,955.3	11.0	6,160	3.5	1,242	694
aequorea jellyfish	*Aequorea* sp.	64.5	0.1	178	0.1	37	37
smooth lumpsucker	*Aptocyclus ventricosus*	15.2	<0.1	7	<0.1	7	7
chum salmon	*Oncorhynchus keta*	13.0	<0.1	5	<0.1	5	5
aurelia jellyfish	*Aurelia* sp.	10.4	<0.1	59	<0.1	33	33
Pacific cod	*Gadus macrocephalus*	8.5	<0.1	4	<0.1	3	3
Pacific herring	*Clupea pallasii*	7.3	<0.1	27	<0.1	27	27
egg yolk jelly	*Phacellophora camtschatica*	5.3	<0.1	23	<0.1	20	20
lumpsuckers	Cyclopteridae (family)	3.3	<0.1	1	<0.1	1	1
sockeye salmon	*Oncorhynchus nerka*	3.3	<0.1	2	<0.1	2	2
magistrate armhook squid	*Berryteuthis magister*	2.8	<0.1	6	<0.1	5	5
flathead sole	*Hippoglossoides elassodon*	2.6	<0.1	5	<0.1	5	5
arrowtooth flounder	*Atheresthes stomias*	2.6	<0.1	2	<0.1	2	2
snailfishes	Liparidae (family)	2.0	<0.1	1	<0.1	1	1
eulachon	*Thaleichthys pacificus*	1.8	<0.1	23	<0.1	23	23
Chinook salmon	*Oncorhynchus tshawytscha*	1.6	<0.1	1	<0.1	1	1
southern rock sole	*Lepidopsetta bilineata*	1.4	<0.1	3	<0.1	3	3
northern rockfish	*Sebastes polyspinis*	0.9	<0.1	2	<0.1	2	2
jellyfishes	Scyphozoa (class)	0.8	<0.1	20	<0.1	2	2
northern rock sole	*Lepidopsetta polyxystra*	0.7	<0.1	1	<0.1	1	1
rock sole spp.	Lepidopsetta (genus)	0.7	<0.1	2	<0.1	2	2
salmon spp.	Oncorhynchus (genus)	0.6	<0.1	2	<0.1	2	2
Pacific capelin	*Mallotus catervarius*	0.5	<0.1	28	<0.1	28	28
great sculpin	*Myoxocephalus polyacanthocephalus*	0.4	<0.1	1	<0.1	1	1
sturgeon poacher	*Podothecus accipenserinus*	0.2	<0.1	5	<0.1	5	5
pollock age 0	*Gadus chalcogrammus*	0.2	<0.1	1,151	0.7	24	0
squids	Cephalopoda (class)	0.2	<0.1	48	<0.1	25	0
yellowfin sole	*Limanda aspera*	0.2	<0.1	1	<0.1	1	1
Pacific sandfish	*Trichodon trichodon*	0.1	<0.1	1	<0.1	1	1
fish larvae	Actinopterygii (class)	<0.1	<0.1	6	<0.1	4	4
sculpins	Cottidae (family)	<0.1	<0.1	1	<0.1	1	0
Total		44,881.6		174,890		20,523	4,419

Table 5. -- Catch by species and numbers of length and weight measurements taken from three Methot hauls during the 2024 acoustic-trawl survey of the Eastern Bering Sea.

		Catch				Measurements	
Species name	Scientific name	Weight (kg)	%	Number	%	Length	Weight
chrysaora jellyfish	*Chrysaora* sp.	36.4	86.7	474	0.5	105	48
euphausiids	Euphausiacea (order)	4.7	11.1	99,127	99.5	0	0
aurelia jellyfish	*Aurelia* sp.	0.7	1.6	5	<0.1	0	0
jellyfishes	Scyphozoa (class)	0.2	0.5	3	<0.1	3	3
hydromedusas	Hydromedusa (unid.)	<0.1	<0.1	2	<0.1	2	2
amphipods	Amphipoda (order)	<0.1	<0.1	24	<0.1	0	0
Total		42.0		99,635		110	53

Table 6. -- Numbers of specimens measured and biological samples collected during the 2024 EBS acoustic-trawl survey. SCA is the Steller sea lion Conservation Area.

Haul	Region	Pollock age 1+					Pollock age 0		Other	
No.	Name	Lengths	Weights	Maturities	Otoliths	Ovaries	Lengths	Weights	Lengths	Weights
1	East of 170	428	91	66	56	-	-	-	47	47
2	SCA	333	76	65	50	8	-	-	26	26
3	East of 170	419	76	45	50	5	-	-	40	40
4	SCA	411	72	52	50	-	-	-	16	16
5	SCA	131	41	7	12	-	-	-	30	29
6	SCA	305	50	50	50	6	-	-	18	18
7	SCA	134	94	39	44	8	-	-	19	19
8	East of 170	347	50	50	50	1	-	-	36	16
10	East of 170	349	75	75	75	6	-	-	60	35
11	East of 170	428	98	77	82	2	-	-	17	17
12	East of 170	196	70	50	55	3	-	-	14	14
13	East of 170	336	51	50	51	3	-	-	4	4
14	East of 170	407	65	50	50	-	-	-	14	14
15	East of 170	311	50	50	50	5	-	-	66	12
17	West of 170	351	64	64	51	3	-	-	32	32
18	West of 170	298	76	76	50	3	-	-	51	51
19	West of 170	327	50	50	50	-	-	-	52	26
20	West of 170	300	50	50	50	1	-	-	7	7
21	West of 170	326	67	67	54	1	-	-	1	1
22	West of 170	321	50	50	50	1	-	-	28	11
23	West of 170	320	59	50	40	1	-	-	25	25
24	West of 170	426	54	51	40	3	-	-	26	26
25	West of 170	350	50	50	40	3	-	-	40	12
26	West of 170	490	55	50	45	-	-	-	45	15
27	West of 170	376	75	72	45	6	-	-	34	10
29	West of 170	292	50	50	40	3	-	-	4	4
30	West of 170	17	17	17	17	3	-	-	38	13
31	West of 170	409	50	50	40	-	-	-	36	11
32	West of 170	317	50	50	40	1	-	-	26	12
33	West of 170	292	49	49	39	3	-	-	25	15
34	West of 170	402	71	50	46	-	-	-	37	13
35	West of 170	577	67	60	45	7	-	-	46	17
36	West of 170	366	61	61	40	7	-	-	36	10
37	West of 170	342	50	50	40	-	-	-	12	12

Haul No.	Region Name	Pollock age 1+ Lengths	Weights	Maturities	Otoliths	Ovaries	Pollock age 0 Lengths	Weights	Other Lengths	Weights
38	West of 170	671	55	49	45	-	-	-	26	10
39	West of 170	277	52	52	42	-	-	-	14	14
41	West of 170	281	50	50	40	-	-	-	15	15
43	West of 170	417	51	50	41	-	-	-	23	11
44	West of 170	348	126	113	50	-	-	-	21	21
45	West of 170	319	122	106	50	-	-	-	32	13
46	West of 170	341	73	73	45	5	-	-	19	19
47	West of 170	312	50	50	40	-	-	-	24	12
48	West of 170	396	147	77	50	7	-	-	25	25
50	West of 170	524	113	73	44	-	-	-	23	23
51	West of 170	338	51	51	26	-	-	-	22	13
52	West of 170	437	51	51	25	-	-	-	30	15
53	West of 170	290	50	50	25	-	-	-	15	10
54	West of 170	431	50	50	25	-	-	-	30	12
55	West of 170	292	50	50	25	-	-	-	18	10
57	West of 170	311	50	50	-	-	-	-	33	13
58	West of 170	455	83	62	25	-	-	-	51	15
59	West of 170	316	50	50	25	-	-	-	7	7
60	West of 170	307	51	51	26	1	-	-	17	10
61	West of 170	403	52	52	25	-	-	-	34	15
65	West of 170	107	50	50	25	-	24	-	5	5
Total		19,007	3,501	3,053	2,286	106	24	0	1,492	918

Table 7. -- Numbers-at-length estimates (millions of fish) from acoustic-trawl surveys of walleye pollock in the core area of the Eastern Bering Sea.

Length	1994	1996	1997	1999	2000	2002	2004	2006	2007	2008	2009	2010	2012	2014	2016	2018	2022	2024
5	<1	<1	<1	<1	<1	<1	<1	<1	<1	<1	<1	<1	<1	<1	<1	<1	<1	0
6	<1	<1	<1	<1	<1	<1	<1	<1	<1	<1	<1	<1	<1	<1	<1	<1	<1	0
7	<1	<1	<1	<1	<1	<1	<1	<1	<1	<1	<1	<1	<1	<1	<1	<1	<1	0
8	<1	<1	<1	<1	<1	<1	<1	<1	<1	<1	<1	<1	<1	<1	<1	<1	<1	0
9	<1	2.6	4.7	1.6	1.1	<1	<1	<1	<1	<1	5.4	<1	<1	<1	<1	<1	<1	<1
10	9.4	25.0	25.2	7.8	5.2	2.7	<1	2.9	32.6	<1	48.9	<1	1.6	3.6	<1	<1	3.6	<1
11	19.6	83.3	52.2	31.5	10.5	8.2	1.0	9.3	268.9	1.7	228.2	1.1	8.3	24.6	2.5	<1	7.8	264.1
12	46.2	104.2	109.8	55.0	20.5	16.2	4.9	64.7	680.2	5.0	779.8	9.5	13.7	95.2	6.8	2.7	14.8	1012.3
13	97.3	137.2	398.7	69.6	41.5	40.9	7.4	150.6	1360.7	11.5	1127.7	68.7	16.4	511.5	19.1	10.2	20.5	1659.9
14	173.9	148.0	1517.9	93.0	65.4	130.4	14.2	126.7	1529.0	15.5	1103.3	267.0	24.9	966.9	28.3	26.1	28.0	1206.9
15	245.9	224.9	3064.7	88.4	81.4	225.4	11.2	92.7	824.7	10.5	1061.1	516.8	31.8	1183.0	34.3	55.8	21.8	519.1
16	206.5	287.3	3432.4	62.8	95.3	202.0	12.2	32.9	577.9	6.4	543.3	807.9	25.0	964.2	24.9	95.7	13.4	271.8
17	139.5	349.9	2241.8	34.0	57.7	110.7	9.7	11.6	310.6	7.8	270.3	705.0	14.7	585.8	18.8	98.0	12.4	88.3
18	149.7	228.9	1326.8	23.3	25.0	39.9	6.0	4.2	117.8	47.7	85.7	305.6	9.3	306.3	12.0	96.1	9.7	38.3
19	239.9	118.6	578.2	55.5	34.4	41.9	7.7	5.5	135.3	128.2	84.6	155.9	24.8	106.3	19.6	39.6	8.2	32.4
20	404.8	69.4	184.7	173.9	53.0	64.8	11.5	11.7	118.4	265.7	57.8	175.2	77.5	73.2	33.3	18.5	9.0	75.8
21	617.7	42.1	80.1	280.5	98.6	166.1	26.2	18.0	145.0	410.0	79.4	227.5	188.5	105.1	70.9	11.7	13.0	160.2
22	813.8	72.6	87.4	346.7	142.9	295.5	39.2	32.8	147.4	447.2	109.3	372.9	312.8	213.3	139.3	19.4	19.9	230.9
23	800.4	68.9	157.9	313.5	192.1	492.6	52.3	38.5	129.6	566.5	138.0	625.7	388.2	442.9	179.4	36.7	22.2	244.1
24	780.8	77.9	264.9	240.7	192.1	745.2	53.7	35.2	143.3	446.2	114.5	934.3	356.2	1029.8	205.6	66.3	29.9	171.5
25	589.3	55.9	415.2	178.8	212.3	867.1	43.4	30.8	92.6	353.1	117.1	1165.5	289.5	1745.3	160.5	93.0	30.3	71.3
26	380.4	47.1	468.9	201.8	191.9	839.2	35.9	26.0	66.5	231.4	116.7	1171.4	223.7	1992.6	128.6	130.4	34.7	38.8
27	204.9	41.9	528.8	270.6	190.9	723.7	29.3	22.9	51.4	115.1	132.3	929.4	191.7	1536.7	118.8	109.0	36.6	34.3
28	130.9	68.8	429.2	321.1	172.5	521.2	32.4	26.3	34.9	79.3	143.3	578.8	206.2	959.7	148.3	91.7	45.0	51.3
29	143.9	91.2	303.2	431.1	168.2	497.1	72.7	30.8	22.9	101.5	186.6	274.2	260.9	494.1	175.6	48.1	82.1	61.8
30	149.2	128.3	181.4	446.5	170.5	514.2	93.7	36.1	20.1	129.8	210.4	131.9	304.1	328.6	294.9	23.2	101.7	78.8
31	190.1	191.5	119.9	427.9	172.7	599.6	153.3	43.1	17.2	125.1	258.0	89.8	279.5	220.2	468.5	17.1	162.8	65.7
32	245.1	248.6	84.5	423.3	171.1	551.0	154.6	46.7	36.2	134.8	249.2	104.0	228.3	167.1	634.0	17.8	222.6	57.6
33	247.2	350.1	73.1	383.0	193.8	544.7	182.5	53.2	47.4	120.3	203.0	114.4	192.6	152.9	751.3	25.5	360.5	47.2
34	302.2	415.2	80.0	408.5	229.1	432.7	187.3	71.4	62.7	117.5	157.3	129.4	210.8	122.8	731.7	31.0	565.2	37.7
35	313.8	466.2	104.7	430.0	341.4	301.1	239.8	85.4	76.8	88.3	110.4	163.1	261.5	170.3	697.7	53.8	764.8	45.6
36	345.9	484.7	183.7	448.0	373.6	257.4	305.3	116.2	66.9	46.1	88.7	235.6	338.3	189.8	534.4	93.4	908.2	75.8
37	367.4	408.3	283.7	417.4	428.7	235.7	433.1	124.7	84.0	32.5	65.9	292.5	411.1	247.2	433.9	165.4	977.1	105.0
38	330.7	341.5	401.5	434.2	386.3	255.0	483.7	133.5	81.4	28.3	47.4	391.7	446.9	265.7	502.9	236.7	1049.0	172.3
39	323.6	264.0	498.7	391.5	362.3	247.8	549.4	125.9	90.9	36.8	42.6	416.8	406.5	282.1	732.8	320.7	913.2	295.7
40	347.1	226.3	484.2	332.4	321.3	252.2	522.2	139.8	118.6	31.1	35.1	382.4	349.1	248.9	1011.9	425.0	776.6	409.6
41	308.3	186.1	422.1	272.4	358.8	238.8	540.2	156.2	129.0	33.8	30.6	299.2	232.4	250.5	992.0	496.3	612.2	578.5
42	330.9	176.2	348.1	279.4	356.2	228.6	523.3	176.9	165.9	43.5	29.7	218.5	159.6	274.1	751.5	516.6	433.4	611.1
43	337.0	174.2	262.3	321.2	369.1	230.1	507.5	187.9	219.6	50.2	26.6	147.6	98.4	390.9	493.0	488.6	303.9	565.1
44	311.7	161.9	205.0	394.2	349.7	237.7	455.6	207.3	228.2	63.2	21.1	103.8	90.7	415.0	354.2	376.7	207.0	463.3
45	335.9	150.4	156.9	415.0	345.9	250.4	404.6	199.5	259.6	66.1	26.2	71.0	81.1	480.8	271.4	299.3	118.4	374.3
46	290.4	137.2	126.0	394.0	319.4	244.2	320.2	191.3	260.0	86.1	26.2	51.4	87.3	428.2	210.8	239.5	97.1	322.8
47	246.9	131.8	106.7	322.8	299.4	239.8	262.4	173.8	231.3	83.7	29.2	32.8	83.5	364.6	176.0	180.5	89.3	240.5
48	199.4	132.0	95.9	260.3	244.0	227.8	219.3	163.9	198.7	97.7	40.9	20.5	79.9	271.1	153.4	141.5	83.8	151.7
49	116.1	117.5	76.7	186.8	193.8	206.2	181.7	128.9	172.5	78.2	44.8	17.5	66.4	215.4	126.1	107.0	81.1	121.0
50	95.0	109.6	79.4	145.2	153.2	185.6	140.7	115.6	144.5	74.3	43.4	19.2	55.5	152.9	108.7	71.0	78.1	86.9
51	58.7	108.1	69.2	111.3	115.8	162.3	116.1	91.6	109.9	70.5	43.3	17.4	40.0	122.8	78.8	53.7	68.7	57.5
52	51.9	88.9	68.7	83.5	80.9	134.0	102.8	81.4	90.2	61.1	43.4	16.9	35.7	90.9	59.1	38.4	66.1	41.6
53	35.0	76.6	65.5	75.3	59.4	120.8	80.5	59.0	67.6	46.6	38.3	16.3	26.4	70.0	43.1	26.2	43.4	35.0
54	30.2	61.2	59.9	63.1	42.3	92.1	65.4	48.1	60.8	43.9	38.0	19.1	26.5	50.3	30.8	16.7	39.9	26.2
55	36.0	47.1	52.8	45.8	30.6	69.5	43.0	33.1	41.3	34.8	33.0	15.5	17.9	40.2	20.4	12.9	30.6	16.5
56	26.1	32.4	46.2	36.2	26.6	59.5	34.2	28.7	31.0	27.6	25.2	15.7	15.9	29.2	14.6	8.7	19.3	13.3
57	25.8	25.5	35.7	33.9	18.5	37.5	23.6	22.2	25.5	21.7	19.7	15.8	13.5	26.5	12.0	5.4	12.9	10.0
58	17.9	21.2	35.5	22.9	15.9	29.8	16.1	17.5	15.8	18.1	20.4	14.8	13.8	22.1	6.1	4.2	6.1	6.4
59	14.6	17.1	27.9	18.7	11.8	18.2	13.8	12.9	11.3	17.0	13.6	9.8	11.4	20.5	4.4	2.4	5.2	3.4
60	13.1	17.1	22.1	16.2	7.4	16.7	9.4	9.1	9.0	13.8	11.3	11.8	12.1	14.9	3.5	1.5	4.8	1.8
61	15.2	16.5	23.6	14.4	6.0	10.9	7.6	7.7	5.5	8.1	9.4	10.3	9.2	13.1	2.4	1.5	1.8	1.4
62	8.6	13.2	15.1	9.4	5.2	7.9	4.8	4.4	4.9	9.2	8.6	7.9	9.5	9.6	2.4	<1	1.2	1.1
63	7.5	8.2	11.8	6.2	3.9	4.4	4.1	3.1	3.6	5.7	5.0	5.5	5.9	7.4	2.3	<1	<1	<1
64	4.6	9.9	11.3	4.9	3.4	4.1	1.2	3.5	3.3	4.4	5.1	5.6	7.0	4.6	1.4	<1	1.1	1.1
65	6.3	7.1	8.7	4.9	2.0	3.6	1.0	1.6	2.0	3.1	5.3	3.5	4.1	4.8	1.2	<1	<1	1.7

Length	1994	1996	1997	1999	2000	2002	2004	2006	2007	2008	2009	2010	2012	2014	2016	2018	2022	2024
66	3.0	6.7	6.8	4.5	1.6	2.4	1.2	1.6	1.8	2.4	4.1	3.3	4.2	2.7	<1	<1	<1	<1
67	3.2	3.7	6.4	3.1	<1	1.1	<1	<1	1.3	1.7	2.9	2.3	2.1	1.4	1.3	<1	<1	<1
68	3.7	2.9	4.6	2.2	1.1	<1	<1	<1	<1	1.5	1.9	2.5	2.4	1.2	<1	<1	<1	<1
69	<1	1.8	4.1	1.7	1.2	<1	<1	<1	<1	<1	1.8	<1	<1	1.2	<1	<1	<1	<1
70	2.8	1.8	1.3	1.1	<1	1.2	<1	<1	<1	<1	1.3	<1	1.3	1.2	<1	<1	<1	<1
71	1.8	1.1	1.1	<1	<1	<1	<1	<1	<1	<1	<1	<1	<1	<1	<1	<1	<1	<1
72	1.5	1.1	1.7	<1	<1	<1	<1	<1	<1	<1	<1	<1	<1	<1	<1	<1	<1	<1
73	<1	<1	1.8	<1	<1	<1	<1	<1	<1	<1	<1	<1	<1	<1	<1	<1	<1	<1
74	<1	<1	<1	<1	<1	<1	<1	<1	<1	<1	<1	<1	<1	<1	<1	<1	<1	0
75	<1	<1	<1	<1	<1	<1	<1	<1	<1	<1	<1	<1	<1	<1	<1	<1	<1	0
76	<1	<1	<1	<1	<1	<1	<1	<1	<1	<1	<1	<1	<1	<1	<1	<1	<1	<1
77	<1	<1	<1	<1	<1	<1	<1	<1	<1	<1	<1	<1	<1	<1	<1	<1	<1	<1
78	<1	<1	<1	<1	<1	<1	<1	<1	<1	<1	<1	<1	<1	<1	<1	<1	<1	0
79	<1	<1	<1	<1	<1	<1	<1	<1	<1	<1	<1	<1	<1	<1	<1	<1	<1	0
80	<1	<1	<1	<1	<1	<1	<1	<1	<1	<1	<1	<1	<1	<1	<1	<1	<1	0
81	<1	<1	<1	<1	<1	<1	<1	<1	<1	<1	<1	<1	<1	<1	<1	<1	<1	0
82	<1	<1	<1	<1	<1	<1	<1	<1	<1	<1	<1	<1	<1	<1	<1	<1	<1	0
83	<1	<1	<1	<1	<1	<1	<1	<1	<1	<1	<1	<1	<1	<1	<1	<1	<1	0
84	<1	<1	<1	<1	<1	<1	<1	<1	<1	<1	<1	<1	<1	<1	<1	<1	<1	0
85	<1	<1	<1	<1	<1	<1	<1	<1	<1	<1	<1	<1	<1	<1	<1	<1	<1	0
86	<1	<1	<1	<1	<1	<1	<1	<1	<1	<1	<1	<1	<1	<1	<1	<1	<1	0
87	<1	<1	<1	<1	<1	<1	<1	<1	<1	<1	<1	<1	<1	<1	<1	<1	<1	0
88	<1	<1	<1	<1	<1	<1	<1	<1	<1	<1	<1	<1	<1	<1	<1	<1	<1	0
89	<1	<1	<1	<1	<1	<1	<1	<1	<1	<1	<1	<1	<1	<1	<1	<1	<1	0
90	<1	<1	<1	<1	<1	<1	<1	<1	<1	<1	<1	<1	<1	<1	<1	<1	<1	0
91	<1	<1	<1	<1	<1	<1	<1	<1	<1	<1	<1	<1	<1	<1	<1	<1	<1	0
92	<1	<1	<1	<1	<1	<1	<1	<1	<1	<1	<1	<1	<1	<1	<1	<1	<1	0
93	<1	<1	<1	<1	<1	<1	<1	<1	<1	<1	<1	<1	<1	<1	<1	<1	<1	0
94	<1	<1	<1	<1	<1	<1	<1	<1	<1	<1	<1	<1	<1	<1	<1	<1	<1	0
95	<1	<1	<1	<1	<1	<1	<1	<1	<1	<1	<1	<1	<1	<1	<1	<1	<1	0
Total	12300.4	7920.1	20631.7	11380.3	8628.9	13290.0	7859.7	3880.6	9989.5	5213.0	8655.4	12923.8	7392.5	19516.3	12244.8	5551.9	9674.4	11358.7

Table 8. -- Biomass-at-length estimates (thousands of metric tons) from acoustic-trawl surveys of walleye pollock in the core area of the Eastern Bering Sea.

Length	1994	1996	1997	1999	2000	2002	2004	2006	2007	2008	2009	2010	2012	2014	2016	2018	2022	2024
5	<1	<1	<1	<1	<1	<1	<1	<1	<1	<1	<1	<1	<1	<1	<1	<1	<1	0
6	<1	<1	<1	<1	<1	<1	<1	<1	<1	<1	<1	<1	<1	<1	<1	<1	<1	0
7	<1	<1	<1	<1	<1	<1	<1	<1	<1	<1	<1	<1	<1	<1	<1	<1	<1	0
8	<1	<1	<1	<1	<1	<1	<1	<1	<1	<1	<1	<1	<1	<1	<1	<1	<1	0
9	<1	<1	<1	<1	<1	<1	<1	<1	<1	<1	<1	<1	<1	<1	<1	<1	<1	<1
10	<1	<1	<1	<1	<1	<1	<1	<1	<1	<1	<1	<1	<1	<1	<1	<1	<1	<1
11	<1	<1	<1	<1	<1	<1	<1	<1	2.5	<1	2.1	<1	<1	<1	<1	<1	<1	2.3
12	<1	1.4	1.4	<1	<1	<1	<1	<1	7.5	<1	9.3	<1	<1	1.1	<1	<1	<1	11.9
13	1.5	2.3	6.8	1.2	<1	<1	<1	2.4	19.5	<1	17.4	1.1	<1	7.9	<1	<1	<1	23.5
14	3.5	3.1	33.3	1.9	1.4	3.0	<1	2.3	26.3	<1	21.9	5.6	<1	18.1	<1	<1	<1	21.5
15	6.1	5.9	84.5	2.1	2.1	6.5	<1	2.2	18.2	<1	26.0	13.2	<1	27.8	<1	1.2	<1	11.1
16	6.2	8.9	113.3	2.0	3.1	7.0	<1	<1	15.2	<1	16.4	25.4	<1	27.3	<1	2.6	<1	7.0
17	5.0	13.0	85.7	1.3	2.3	4.6	<1	<1	10.1	<1	10.3	26.4	<1	19.8	<1	3.1	<1	2.9
18	6.4	10.1	59.0	1.1	1.2	1.9	<1	<1	4.5	1.8	3.7	13.4	<1	12.4	<1	3.8	<1	1.4
19	12.0	6.1	29.2	3.1	1.9	2.4	<1	<1	6.3	5.9	4.3	7.6	1.2	4.9	<1	1.8	<1	1.4
20	23.5	4.2	10.9	11.0	3.3	4.2	<1	<1	6.4	14.1	3.3	10.0	4.1	4.0	1.7	<1	<1	4.0
21	41.5	2.9	5.3	20.4	7.2	12.5	1.8	1.2	9.8	25.1	5.4	15.4	11.7	6.6	4.3	<1	<1	9.8
22	62.6	5.8	6.6	28.8	11.9	25.2	3.0	2.5	11.6	32.5	8.8	29.6	22.3	16.0	10.0	1.4	1.4	16.3
23	70.1	6.2	13.6	29.6	18.1	47.9	4.7	3.3	11.5	47.9	12.5	56.5	32.8	40.6	14.4	3.1	1.8	19.7
24	77.4	8.0	25.9	25.5	20.5	82.3	5.4	3.4	14.6	42.8	11.7	97.0	34.3	108.3	19.4	6.1	2.7	15.4
25	65.8	6.5	45.9	21.2	25.4	108.5	4.9	3.2	10.3	38.1	14.3	137.2	31.3	209.9	16.9	10.0	3.1	7.2
26	47.7	6.1	58.3	26.8	25.6	118.5	4.7	3.2	8.1	28.1	15.7	154.0	27.1	270.0	15.3	15.9	4.1	4.5
27	28.7	6.1	73.7	39.9	28.4	114.2	4.3	3.1	7.0	15.7	20.8	136.3	26.3	231.3	16.2	15.2	4.9	4.5
28	20.4	11.1	66.7	52.5	28.5	90.5	5.3	4.0	5.3	12.0	24.3	95.7	31.4	157.5	22.6	14.2	6.6	7.5
29	25.0	16.3	52.5	77.8	30.6	93.9	13.2	5.2	3.9	17.0	36.8	49.7	44.9	89.8	29.6	8.5	13.8	10.1
30	28.5	25.4	34.9	88.5	34.2	105.4	18.6	6.7	3.8	23.9	45.0	25.4	57.0	65.4	54.3	4.4	19.2	14.2
31	40.2	41.7	25.6	92.9	38.0	134.0	33.6	9.4	3.6	25.8	61.7	19.6	59.2	47.4	97.3	3.6	33.6	13.3
32	56.6	59.5	19.8	100.3	41.1	134.0	37.0	11.0	8.8	30.4	64.9	25.0	52.5	39.7	146.4	4.1	51.0	12.7
33	62.4	91.7	18.7	98.9	50.8	144.4	48.8	13.6	12.4	30.0	57.8	30.7	48.0	39.8	189.9	6.4	91.1	11.5
34	82.9	118.8	22.4	114.6	65.4	125.1	54.0	19.9	18.0	31.3	48.4	38.6	57.3	34.9	202.5	8.6	153.4	9.9
35	93.7	145.2	31.8	130.7	105.8	95.1	74.7	26.0	24.0	26.4	36.7	53.0	77.1	53.4	211.6	16.2	223.9	13.4
36	112.2	164.0	60.9	147.3	125.4	88.2	104.2	38.3	22.5	15.1	31.6	83.1	108.9	65.5	178.2	31.6	291.6	23.7
37	129.0	149.7	102.5	148.1	155.6	87.6	157.8	43.3	31.0	11.5	24.6	111.6	144.3	91.8	158.3	60.1	341.2	36.4
38	125.6	135.5	156.9	165.9	151.1	100.9	190.7	50.8	32.4	10.8	19.5	163.8	166.5	106.8	205.1	92.8	395.2	65.0
39	133.1	112.9	210.8	160.7	152.4	105.4	233.1	51.9	38.9	15.1	18.2	185.0	163.5	121.2	327.7	134.5	378.3	120.4
40	153.6	104.3	220.6	146.2	145.6	114.9	240.1	61.2	53.7	13.9	16.2	183.8	151.4	115.3	490.6	189.9	348.4	176.7
41	147.3	92.1	207.3	128.3	174.5	116.3	265.6	73.0	62.4	16.0	15.5	153.4	107.9	124.9	514.1	235.2	295.0	266.1
42	171.2	93.8	184.0	140.9	185.8	118.8	276.3	89.6	84.9	21.5	16.1	119.1	79.5	145.5	410.5	263.3	222.9	301.9
43	188.9	99.1	148.5	172.6	205.9	128.5	290.7	100.3	121.6	27.3	15.4	85.5	52.3	222.5	281.1	265.7	162.4	293.7
44	188.8	98.8	124.3	225.8	208.1	140.9	278.1	119.4	133.3	36.2	13.0	63.9	51.4	250.5	212.3	219.5	117.3	260.5
45	219.0	98.1	101.7	252.4	218.2	157.9	261.4	121.1	162.4	40.5	16.6	46.2	49.4	308.0	170.8	186.9	68.6	224.4
46	202.0	95.3	87.3	254.8	214.4	164.5	217.5	123.3	174.5	55.6	18.3	35.9	56.3	290.9	138.2	156.5	60.0	204.8
47	182.7	97.7	78.7	221.0	211.9	171.4	188.4	119.1	163.2	57.7	21.6	24.0	58.1	261.8	119.7	124.4	59.1	162.5
48	156.1	104.9	75.6	189.0	183.1	173.1	164.4	117.9	149.7	69.8	32.3	16.3	59.5	205.4	110.9	101.5	58.1	108.7
49	96.3	98.6	64.5	143.8	153.6	167.1	143.7	98.6	136.0	60.1	37.0	14.6	52.2	172.2	95.6	81.1	59.4	90.6
50	83.6	97.7	71.2	118.3	128.1	157.9	117.9	95.4	121.9	60.9	38.5	16.9	45.7	129.1	86.2	56.5	61.0	66.4
51	54.5	102.5	65.9	95.3	101.9	146.7	102.8	78.5	97.2	60.0	40.2	16.4	35.4	110.6	66.0	44.5	56.8	48.3
52	51.5	89.3	69.0	75.8	74.7	128.5	95.2	73.2	84.9	56.3	42.9	16.7	32.6	87.2	51.9	32.9	59.3	35.7
53	36.5	81.4	69.6	71.9	58.5	123.5	79.2	57.2	66.1	46.0	39.2	16.8	26.3	70.1	39.6	24.2	41.7	32.0
54	33.6	68.5	67.7	63.5	42.7	98.4	67.7	49.2	64.6	44.8	41.5	20.9	27.8	53.4	30.2	16.1	39.1	26.5
55	42.4	55.8	62.6	48.5	33.1	78.3	46.3	35.8	46.6	38.2	37.7	17.8	19.9	45.0	21.5	13.3	31.7	17.8
56	32.6	40.8	58.3	40.7	29.9	70.9	39.5	31.4	36.6	32.9	30.8	19.4	18.1	34.3	15.8	9.6	21.4	15.6
57	34.1	34.1	48.0	40.1	21.9	46.9	29.0	26.3	32.1	26.6	26.0	19.9	16.4	32.3	13.9	6.4	14.8	12.1
58	25.1	29.9	51.0	28.7	19.5	39.5	20.1	22.0	20.6	24.0	27.3	19.8	17.6	28.7	7.5	5.2	7.4	7.9
59	21.2	25.4	42.0	24.3	15.5	25.2	18.9	17.1	15.9	23.0	20.0	14.2	14.8	28.5	5.9	3.1	6.9	4.5
60	19.9	26.1	35.0	22.4	10.2	24.2	13.4	13.0	13.2	20.5	17.3	18.1	17.2	21.5	4.7	2.0	6.8	2.4
61	24.3	27.1	39.7	20.9	8.6	16.5	11.7	11.2	8.4	12.5	15.2	16.7	13.5	19.8	3.6	2.1	2.6	2.0
62	14.4	22.9	27.0	14.6	7.9	12.5	7.5	6.9	7.8	15.2	14.2	13.1	15.0	15.8	3.7	1.1	1.9	1.6
63	13.3	14.6	20.7	9.9	6.2	7.3	6.9	5.0	6.3	9.6	8.8	9.6	9.6	12.2	3.8	1.1	<1	1.0
64	8.5	18.4	21.2	8.4	5.6	7.1	2.1	5.9	5.9	7.5	9.3	10.4	11.9	8.2	2.4	1.1	1.8	1.8
65	12.1	13.8	17.0	8.6	3.4	6.7	1.8	2.9	3.7	5.6	10.2	6.9	7.5	8.7	2.2	1.0	<1	3.0

Length	1994	1996	1997	1999	2000	2002	2004	2006	2007	2008	2009	2010	2012	2014	2016	2018	2022	2024
66	6.1	13.7	14.0	8.1	3.0	4.4	2.3	3.1	3.6	4.5	8.2	7.0	7.9	5.5	1.3	<1	<1	<1
67	6.7	7.9	13.7	5.9	1.2	2.1	1.4	1.4	2.6	3.5	6.1	4.9	4.2	2.8	2.7	<1	1.1	<1
68	8.0	6.5	10.2	4.4	2.2	1.9	1.2	1.0	1.8	3.1	4.1	5.8	4.9	2.7	<1	<1	<1	<1
69	2.0	4.3	9.5	3.6	2.5	<1	<1	<1	<1	1.3	4.2	1.7	1.9	2.5	1.7	<1	<1	<1
70	6.4	4.4	3.2	2.4	<1	2.6	<1	<1	2.3	1.7	3.1	2.2	2.9	2.9	<1	<1	2.0	<1
71	4.6	2.9	2.9	2.3	<1	<1	<1	<1	1.2	<1	2.0	<1	1.4	<1	<1	<1	<1	<1
72	3.8	3.0	4.5	1.9	1.3	<1	<1	1.2	<1	1.8	1.9	1.8	1.1	1.6	<1	<1	1.6	<1
73	2.1	1.8	4.9	2.3	<1	<1	<1	<1	<1	<1	1.7	2.6	<1	<1	<1	<1	<1	1.2
74	<1	2.1	1.5	2.4	<1	<1	<1	<1	<1	<1	1.4	1.1	1.3	<1	<1	<1	<1	0
75	1.8	<1	2.8	<1	<1	<1	<1	<1	<1	<1	1.6	<1	<1	<1	<1	<1	<1	0
76	<1	<1	1.0	<1	<1	<1	<1	<1	<1	<1	<1	<1	<1	<1	<1	<1	<1	<1
77	<1	<1	<1	<1	<1	<1	<1	<1	<1	<1	<1	<1	<1	<1	<1	<1	<1	<1
78	1.9	<1	<1	<1	<1	<1	<1	<1	<1	<1	<1	<1	<1	<1	<1	<1	<1	0
79	<1	<1	<1	1.6	<1	<1	<1	<1	<1	<1	<1	<1	<1	<1	<1	<1	<1	0
80	<1	1.2	<1	<1	<1	<1	<1	<1	<1	<1	<1	<1	<1	<1	<1	<1	<1	0
81	<1	<1	<1	<1	<1	<1	<1	<1	<1	<1	<1	<1	<1	<1	<1	<1	<1	0
82	<1	<1	<1	<1	<1	<1	<1	<1	<1	<1	<1	<1	<1	<1	<1	<1	<1	0
83	<1	<1	<1	<1	<1	<1	<1	<1	<1	<1	<1	<1	<1	<1	<1	<1	<1	0
84	<1	<1	<1	<1	<1	<1	<1	<1	<1	<1	<1	<1	<1	<1	<1	<1	<1	0
85	<1	<1	<1	<1	<1	<1	<1	<1	<1	<1	<1	<1	<1	<1	<1	<1	<1	0
86	<1	<1	<1	<1	<1	<1	<1	<1	<1	<1	<1	<1	<1	<1	<1	<1	<1	0
87	<1	<1	<1	<1	<1	<1	<1	<1	<1	<1	<1	<1	<1	<1	<1	<1	<1	0
88	<1	<1	<1	<1	<1	<1	<1	<1	<1	<1	<1	<1	<1	<1	<1	<1	<1	0
89	<1	<1	<1	<1	<1	<1	<1	<1	<1	<1	<1	<1	<1	<1	<1	<1	<1	0
90	<1	<1	<1	<1	<1	<1	<1	<1	<1	<1	<1	<1	<1	<1	<1	<1	<1	0
91	<1	<1	<1	<1	<1	<1	<1	<1	<1	<1	<1	<1	<1	<1	<1	<1	<1	0
92	<1	<1	<1	<1	<1	<1	<1	<1	<1	<1	<1	<1	<1	<1	<1	<1	<1	0
93	<1	<1	<1	<1	<1	<1	<1	<1	<1	<1	<1	<1	<1	<1	<1	<1	<1	0
94	<1	<1	<1	<1	<1	<1	<1	<1	<1	<1	<1	<1	<1	<1	<1	<1	<1	0
95	<1	<1	<1	<1	<1	<1	<1	<1	<1	<1	<1	<1	<1	<1	<1	<1	<1	0
Total	3627.7	2951.7	3587.6	4199.7	3614.7	4301.2	3995.7	1874.1	2282.7	1404.5	1331.4	2635.7	2279.4	4742.8	4837.7	2497.3	3834.0	2875.0

Table 9. -- Estimates of walleye pollock biomass (millions of metric tons) and relative estimation error from acoustic-trawl surveys in the core area of the Eastern Bering Sea.

			SCA		East of 170		West of 170		EBS	
Year	Dates	Area (nmi^2)	Biomass	%	Biomass	%	Biomass	%	Biomass	Est. error
1994	9 Jul - 7 Sept	78,251	0.382	10.5	0.652	18.0	2.594	71.5	3.628	4.0%
1996	20 Jul - 30 Aug	93,810	0.275	9.3	0.492	16.7	2.185	74.0	2.952	3.2%
1997	17 Jul - 5 Sept	102,770	0.272	7.9	0.703	20.4	2.470	71.7	3.588	2.9%
1999	12 Jun - 29 Jul	103,670	0.383	9.1	0.757	18.0	3.060	72.9	4.200	4.4%
2000	12 Jun - 1 Aug	106,140	0.458	12.7	0.715	19.8	2.441	67.5	3.615	2.8%
2002	9 Jun - 21 Jul	99,526	0.762	17.7	0.938	21.8	2.601	60.5	4.301	2.7%
2004	4 Jun - 29 Jul	99,659	0.550	13.8	0.918	23.0	2.528	63.3	3.996	3.1%
2006	3 Jun - 25 Jul	89,550	0.147	7.8	0.340	18.2	1.387	74.0	1.874	3.3%
2007	2 Jun - 30 Jul	92,944	0.136	6.0	0.245	10.7	1.902	83.3	2.283	3.8%
2008	2 Jun - 31 Jul	95,374	0.122	8.7	0.087	6.2	1.196	85.1	1.404	5.6%
2009	9 Jun - 7 Aug	91,414	0.156	11.7	0.058	4.4	1.117	83.9	1.331	6.9%
2010	5 Jun - 7 Aug	92,849	0.098	3.7	0.193	7.3	2.345	89.0	2.636	5.4%
2012	7 Jun - 10 Aug	96,852	0.196	8.6	0.319	14.0	1.764	77.4	2.279	3.4%
2014	12 Jun - 13 Aug	94,361	0.571	12.0	1.458	30.7	2.714	57.2	4.743	3.4%
2016	12 Jun - 17 Aug	100,674	0.542	11.2	1.268	26.2	3.028	62.6	4.838	1.9%
2018	12 Jun - 22 Aug	92,283	0.234	9.4	0.510	20.4	1.753	70.2	2.497	3.9%
2020	4 Jul - 20 Aug	102,320	0.398	11.0	0.531	14.7	2.688	74.3	3.617	9.6%
2022	1 Jun - 5 Aug	103,942	0.538	14.0	0.823	21.5	2.473	64.5	3.834	6.8%
2024	5 Jun - 22 Jul	103,365	0.497	17.3	0.593	20.6	1.785	62.1	2.871	5.6%

Table 10. -- Numbers-at-age estimates (millions of fish) from acoustic-trawl surveys of walleye pollock in the core area of the Eastern Bering Sea.

Age	1994	1996	1997	1999	2000	2002	2004	2006	2007	2008	2009	2010	2012	2014	2016	2018	2022	2024
1	955.8	1579.9	12974.5	451.7	382.3	752.1	67.8	499.1	5726.2	57.4	5207.8	2560.8	145.1	4697.3	163.1	411.8	141.6	5052.1
2	4929.5	552.1	2860.8	1770.8	1318.8	4928.9	314.8	214.8	1034.5	2901.0	818.2	6377.3	1954.5	8704.4	1037.6	521.8	332.3	1028.0
3	1420.7	550.8	435.8	3716.6	1222.4	3379.4	1218.3	289.4	339.4	1053.0	1742.6	978.1	1663.8	966.8	4501.3	254.5	975.2	715.7
4	1784.1	2738.9	536.1	1803.5	2577.9	1289.0	3106.7	649.1	473.0	165.4	285.0	2288.1	2705.1	1146.1	4499.6	606.7	6577.7	346.7
5	2223.0	915.0	2355.3	649.2	1004.6	660.2	1624.9	781.3	791.7	156.7	76.1	448.2	282.3	1105.8	719.3	2295.2	819.4	1031.6
6	444.0	638.0	560.4	403.7	326.0	939.2	567.8	659.2	734.5	282.0	92.6	74.0	371.2	1805.3	348.1	951.6	211.0	2516.8
7	129.5	596.7	324.7	1586.1	309.0	541.0	288.5	393.8	412.0	235.2	130.2	33.1	114.3	758.3	398.1	200.3	133.0	395.2
8	133.9	146.1	302.3	548.1	957.4	142.5	283.6	146.7	245.3	138.5	112.0	36.4	35.6	169.5	427.8	112.0	239.1	106.7
9	67.1	40.4	76.3	190.6	281.0	164.5	122.8	75.6	98.8	103.1	77.3	38.0	24.0	76.8	94.3	102.7	166.3	58.7
10	65.9	29.5	28.0	157.0	136.5	307.8	69.0	59.3	39.4	32.9	44.6	29.1	27.6	29.5	28.9	69.7	33.9	64.2
11	29.7	22.6	30.6	49.5	59.8	105.2	58.9	33.0	37.4	30.2	26.0	25.9	23.8	11.1	15.9	17.1	16.7	25.8
12	52.6	39.4	33.5	22.2	35.3	44.5	77.5	21.7	19.4	19.6	11.2	13.2	16.9	11.9	4.4	4.9	17.9	6.8
13	16.9	13.5	35.7	8.5	6.3	19.3	37.0	16.3	8.9	10.7	10.1	7.9	14.9	11.7	2.4	2.6	6.6	9.2
14	17.6	24.1	17.6	6.1	4.0	11.0	11.8	19.7	9.3	5.6	5.1	4.7	4.6	6.5	1.4	<1	2.1	<1
15	7.6	10.1	23.7	3.9	3.3	1.1	8.9	9.9	10.2	5.8	3.7	3.2	3.5	5.5	2.3	<1	1.6	<1
16	13.2	11.3	13.7	3.5	1.4	<1	<1	6.5	4.7	7.8	3.4	1.2	1.4	3.6	<1	<1	<1	0
17	7.4	5.5	16.0	3.7	1.4	<1	<1	2.0	<1	3.6	2.5	<1	<1	2.7	<1	<1	<1	<1
18	<1	4.2	2.0	1.8	1.0	1.0	<1	<1	1.5	1.6	2.3	2.0	<1	1.6	<1	<1	<1	0
19	<1	2.0	2.3	3.1	<1	<1	<1	2.5	1.0	2.4	1.6	<1	<1	<1	<1	<1	<1	0
20	<1	<1	2.4	<1	<1	<1	<1	<1	<1	<1	2.3	<1	<1	<1	<1	<1	<1	0
21	<1	<1	<1	<1	<1	<1	<1	<1	<1	<1	<1	<1	<1	<1	<1	<1	<1	0
22	<1	<1	<1	<1	<1	<1	<1	<1	<1	<1	<1	<1	<1	<1	<1	<1	<1	0
23	<1	<1	<1	<1	<1	<1	<1	<1	<1	<1	<1	<1	<1	<1	<1	<1	<1	0
24	<1	<1	<1	<1	<1	<1	<1	<1	<1	<1	<1	<1	<1	<1	<1	<1	<1	0
25	<1	<1	<1	<1	<1	<1	<1	<1	<1	<1	<1	<1	<1	<1	<1	<1	<1	0
26	<1	<1	<1	<1	<1	<1	<1	<1	<1	<1	<1	<1	<1	<1	<1	<1	<1	0
27	<1	<1	<1	<1	<1	<1	<1	<1	<1	<1	<1	<1	<1	<1	<1	<1	<1	0
28	<1	<1	<1	<1	<1	<1	<1	<1	<1	<1	<1	<1	<1	<1	<1	<1	<1	0
29	<1	<1	<1	<1	<1	<1	<1	<1	<1	<1	<1	<1	<1	<1	<1	<1	<1	0
Total	12299.1	7920.1	20631.7	11380.3	8628.8	13290.0	7859.7	3880.6	9989.5	5213.0	8655.4	12923.8	7392.5	19516.3	12244.8	5551.9	9674.4	11358.5

Table 11. -- Biomass-at-age estimates (thousands of tons) from acoustic-trawl surveys of walleye pollock in the core area of the Eastern Bering Sea.

Age	1994	1996	1997	1999	2000	2002	2004	2006	2007	2008	2009	2010	2012	2014	2016	2018	2022	2024
1	24.6	48.7	430.1	10.6	10.4	23.4	1.7	9.5	105.6	1.2	105.8	80.9	2.9	118.1	4.4	12.7	3.2	81.3
2	435.4	42.7	379.3	171.3	147.4	651.2	35.9	21.6	90.4	241.6	80.0	748.3	181.4	1172.0	106.3	60.3	54.2	79.2
3	333.5	123.7	113.0	872.9	292.9	867.2	338.2	70.0	95.4	227.1	417.2	216.9	340.0	218.1	1198.4	57.3	273.9	199.9
4	701.1	907.9	206.2	689.1	1014.9	515.7	1440.7	245.9	209.4	67.9	121.3	1015.6	1027.7	453.8	2176.7	240.7	2481.9	141.9
5	1258.7	452.0	1120.2	303.5	543.3	373.9	932.0	413.8	463.9	90.2	46.5	259.3	158.9	608.1	381.9	1173.3	389.5	506.2
6	296.3	437.8	355.5	244.9	204.4	637.3	397.8	429.0	512.5	196.9	74.2	56.2	272.5	1244.7	218.2	568.6	120.0	1371.2
7	94.8	508.9	264.4	1044.3	217.8	426.1	223.8	300.2	330.8	191.8	121.5	33.6	96.8	565.4	280.5	132.2	97.5	252.6
8	119.0	133.4	302.4	406.2	711.9	128.1	239.2	124.4	217.9	131.2	116.2	42.5	35.7	164.4	331.0	82.4	192.0	86.0
9	71.2	43.8	89.9	170.5	221.8	161.3	113.7	70.4	96.3	100.6	85.7	47.6	29.8	81.5	76.8	82.1	139.7	50.5
10	78.3	36.3	34.7	154.2	124.1	309.3	66.6	58.7	43.0	38.6	55.5	39.4	35.5	34.0	28.5	61.9	32.4	57.8
11	37.5	32.5	43.4	54.4	64.6	111.2	59.6	33.7	41.6	37.0	33.9	35.8	30.9	15.1	18.5	16.3	18.0	27.1
12	76.2	61.0	52.5	25.4	35.5	48.5	80.5	25.2	22.8	23.8	16.8	19.9	22.7	16.5	6.0	4.9	17.8	7.1
13	25.6	21.7	58.7	12.8	7.6	23.4	39.5	20.0	11.7	14.7	16.4	13.2	21.5	18.0	3.7	2.7	8.0	11.9
14	26.3	40.9	29.9	10.2	6.0	15.6	13.6	24.8	13.3	8.3	9.0	8.2	7.6	9.7	2.3	<1	2.9	<1
15	14.8	16.3	39.4	6.2	5.2	1.7	11.3	12.1	13.4	8.1	6.1	5.8	5.8	8.8	3.8	<1	3.1	<1
16	21.8	21.5	24.6	5.5	2.3	1.3	1.3	7.9	6.6	12.2	6.6	2.3	2.6	5.3	<1	<1	<1	0
17	11.3	10.4	30.2	6.9	2.4	1.1	<1	2.8	1.9	5.5	5.1	2.0	1.7	3.9	<1	<1	<1	<1
18	<1	8.4	4.2	2.9	1.8	1.6	<1	<1	2.5	3.1	4.7	4.4	<1	2.2	<1	<1	<1	0
19	<1	3.7	4.6	6.4	<1	1.5	<1	3.0	1.9	3.6	3.0	1.9	1.6	1.3	<1	<1	<1	0
20	<1	<1	4.6	1.4	<1	<1	<1	<1	<1	<1	3.6	<1	<1	<1	<1	<1	<1	0
21	<1	<1	<1	<1	<1	<1	<1	<1	<1	<1	1.5	<1	1.6	<1	<1	<1	<1	0
22	<1	<1	<1	<1	<1	<1	<1	<1	<1	<1	<1	<1	<1	<1	<1	<1	<1	0
23	<1	<1	<1	<1	<1	<1	<1	<1	<1	<1	<1	<1	<1	<1	<1	<1	<1	0
24	<1	<1	<1	<1	<1	<1	<1	<1	<1	<1	<1	<1	<1	0	<1	<1	<1	0
25	<1	<1	<1	<1	<1	<1	<1	<1	<1	<1	<1	<1	<1	<1	<1	<1	<1	0
26	<1	<1	<1	<1	<1	<1	<1	<1	<1	<1	<1	<1	<1	<1	<1	<1	<1	0
27	<1	<1	<1	<1	<1	<1	<1	<1	<1	<1	<1	<1	<1	<1	<1	<1	<1	0
28	<1	<1	<1	<1	<1	<1	<1	<1	<1	<1	<1	<1	<1	<1	<1	<1	<1	0
29	<1	<1	<1	<1	<1	<1	<1	<1	<1	<1	<1	<1	<1	<1	<1	<1	<1	0
Total	3627.7	2951.7	3587.6	4199.7	3614.7	4301.2	3995.7	1874.1	2282.7	1404.5	1331.4	2635.7	2279.4	4742.8	4837.7	2497.3	3834.0	2874.5

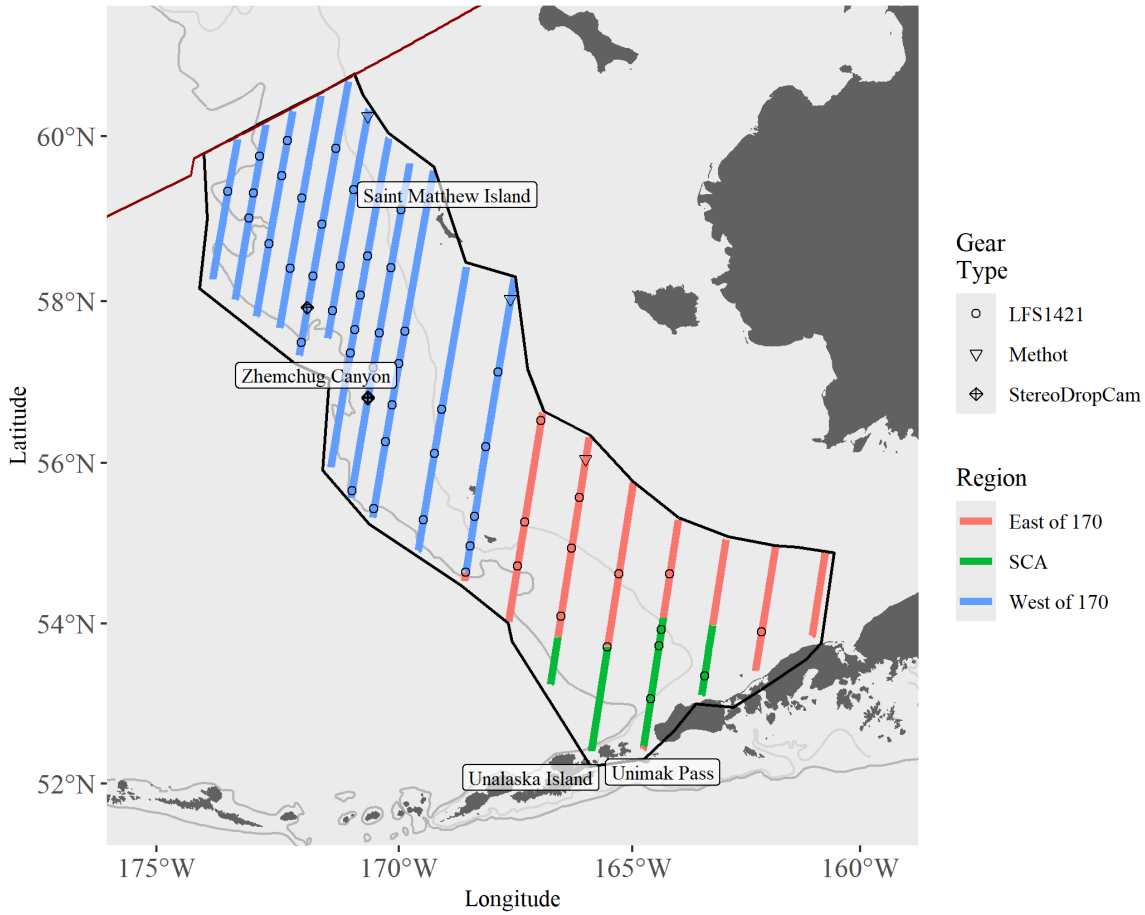

Figure 1. -- Transect lines and locations of trawl hauls during the 2024 Eastern Bering Sea acoustic-trawl survey. The survey region associated with each transect is indicated by the transect color. Locations of trawl events are indicated with black markers. The Steller sea lion Conservation Area (SCA; shown in green) is part of the region east of 170°W and included in summaries of that region. Together, east of 170°W (including the SCA) and west of 170°W comprise the "core area," outlined in black on the map. The U.S.-Russia Convention line is shown in dark red.

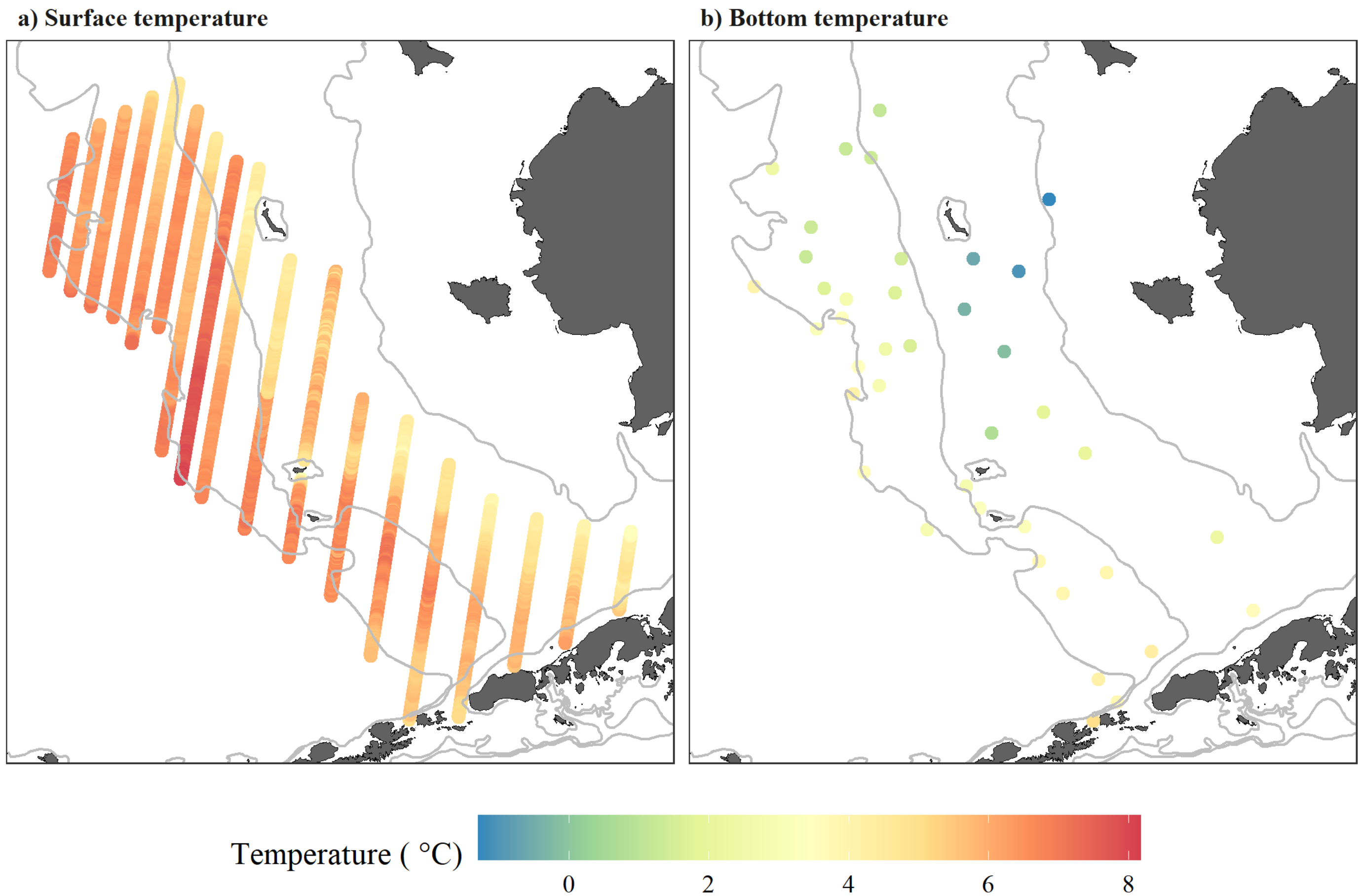

Figure 2. -- Water temperatures (°C) recorded at a) the sea surface at 5-second intervals from the ship's sea surface temperature system and b) near bottom during 40 CTD casts during the summer 2024 acoustic-trawl survey of the Eastern Bering Sea.

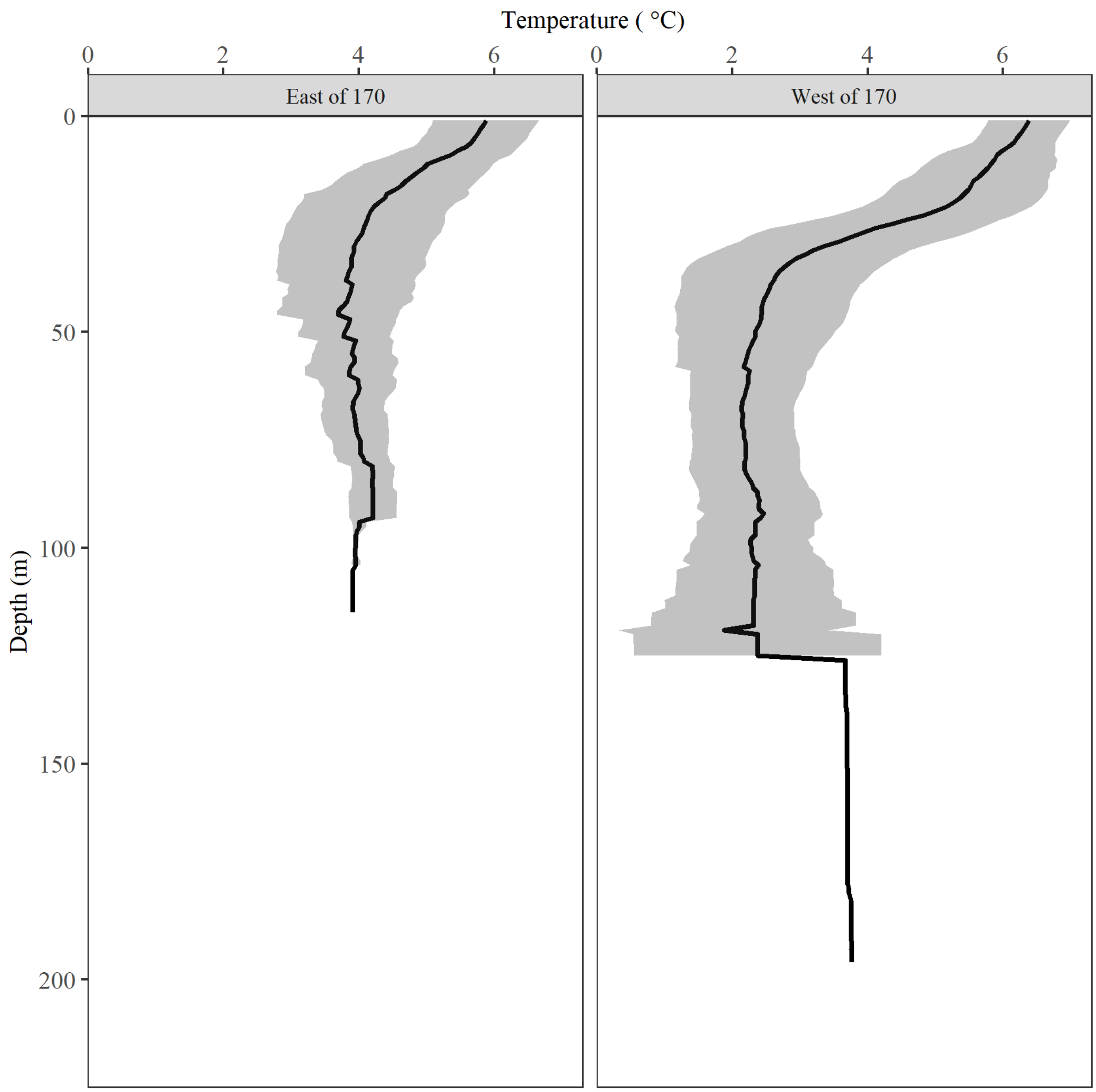

Figure 3. -- Temperature profiles at fishing locations from SBE 39 probes placed on the headrope of fishing gear in the Bering Sea (east and west of 170°W). Black line represents the mean and the gray ribbon represents 1 s.d. east of 170°W includes the Steller sea lion Conservation Area (SCA).

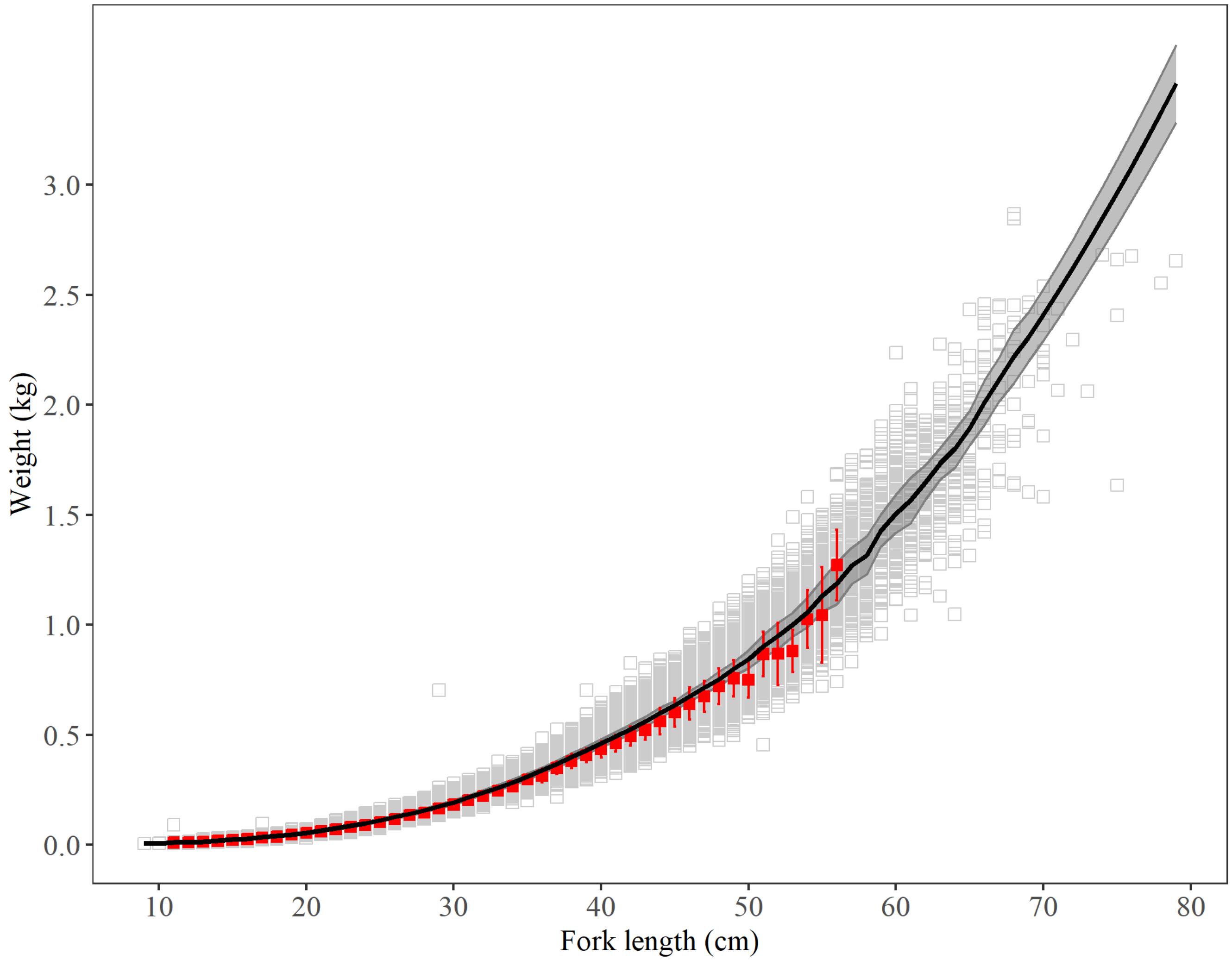

Figure 4. -- Mean weight-at-length for pollock weighed during the Eastern Bering Sea acoustic-trawl survey. The 2024 survey is shown in red (mean +/- 1 s.d). Grey squares indicate the range of observations in previous surveys (2004-2022), and the black line and grey ribbon indicate mean weight at length in previous surveys +/- 1 s.d.

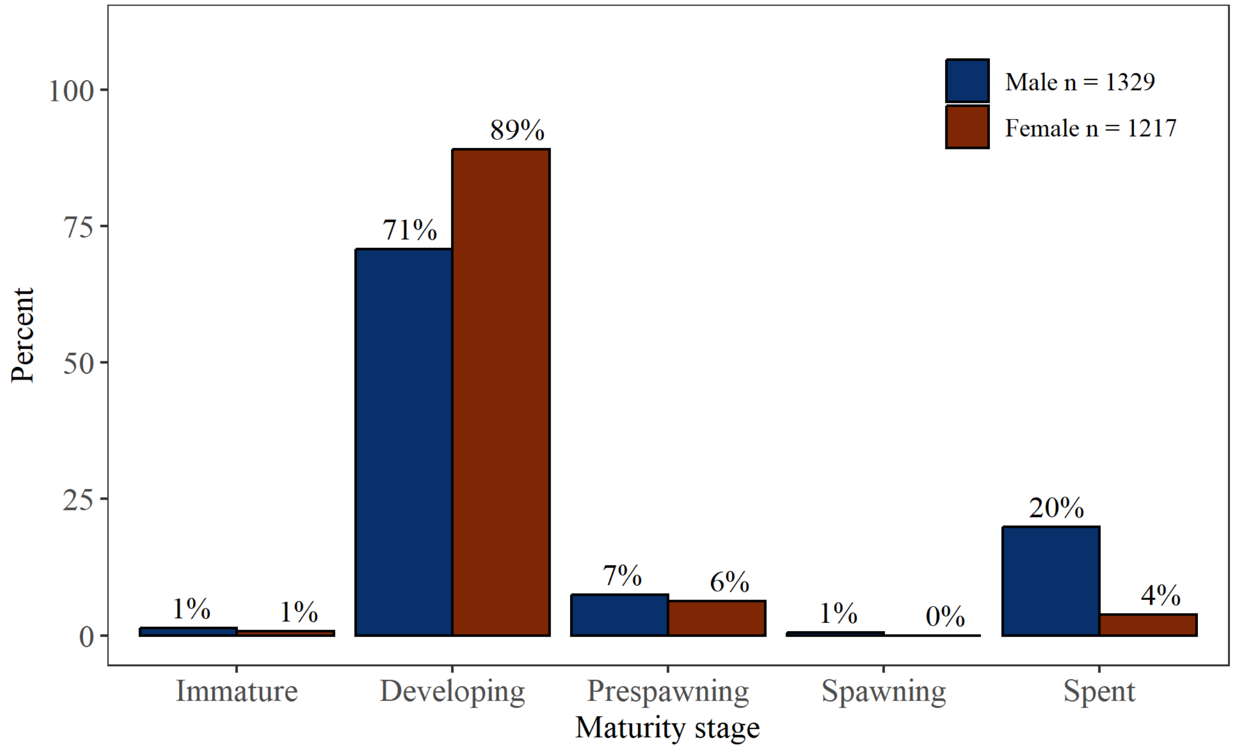

Figure 5. -- Maturity composition for male and female pollock ≥ 34 cm FL within each stage in the 2024 acoustic-trawl survey of the core area of the Eastern Bering Sea. Maturity quantities are weighted by local pollock abundance.

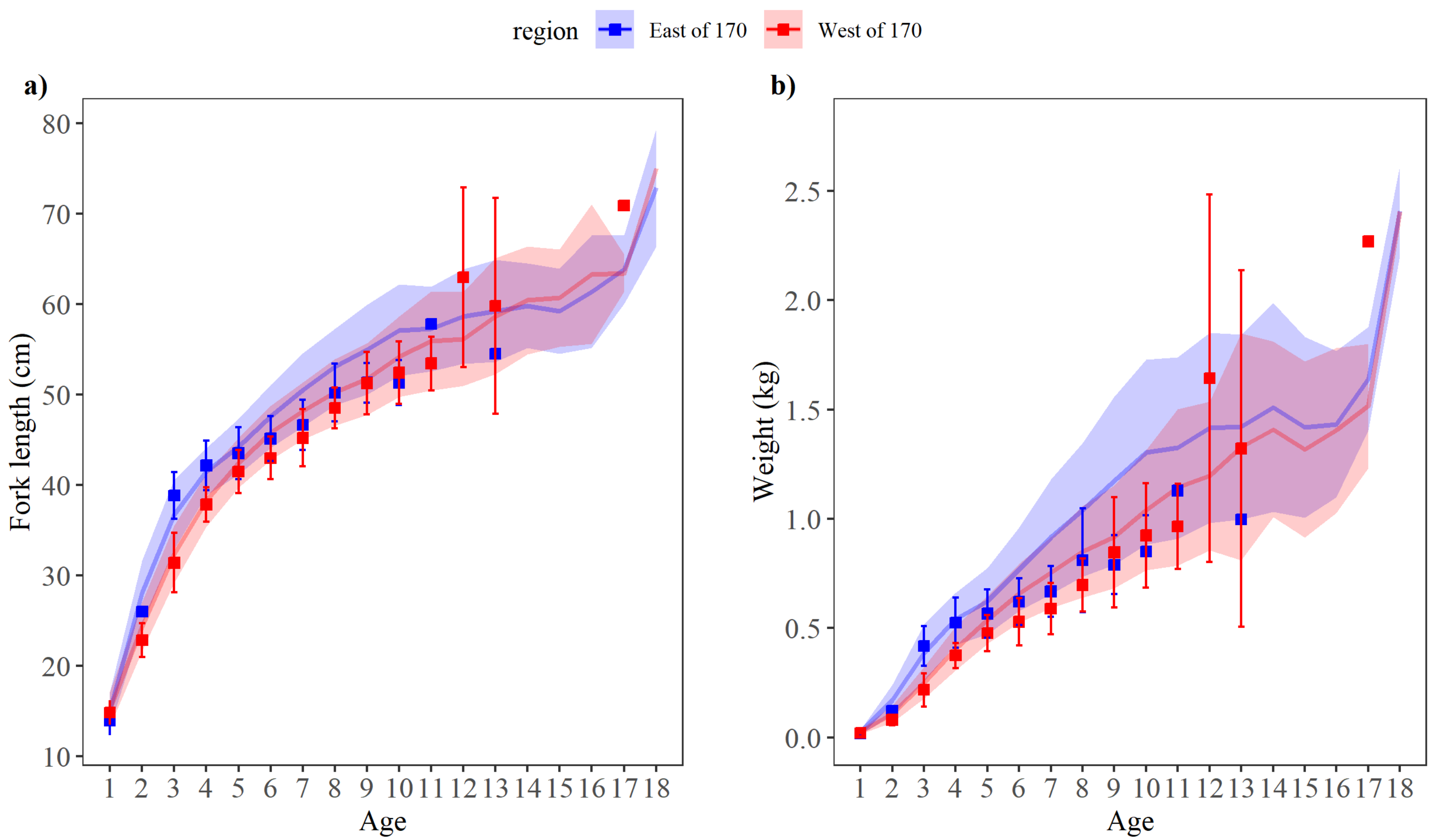

Figure 6. -- Mean length (a), and weight (b) at age for pollock sampled in the AT survey of the core area during summer Eastern Bering Sea surveys. The mean length and weight at age of pollock found east of 170°W (including the Steller sea lion Conservation Area (SCA)) during the 2024 survey are depicted by blue squares, and mean length and weight at age of pollock found west of 170°W are depicted with red squares. Error bars represent mean +/- 1 s.d. The solid lines and shaded regions indicate the mean and +/- 1 s.d., respectively, for observations from 2004 to 2022. East of 170°W (blue) and west of 170°W (red) ribbons indicate mean length at age in historical surveys +/- 1 s.d.

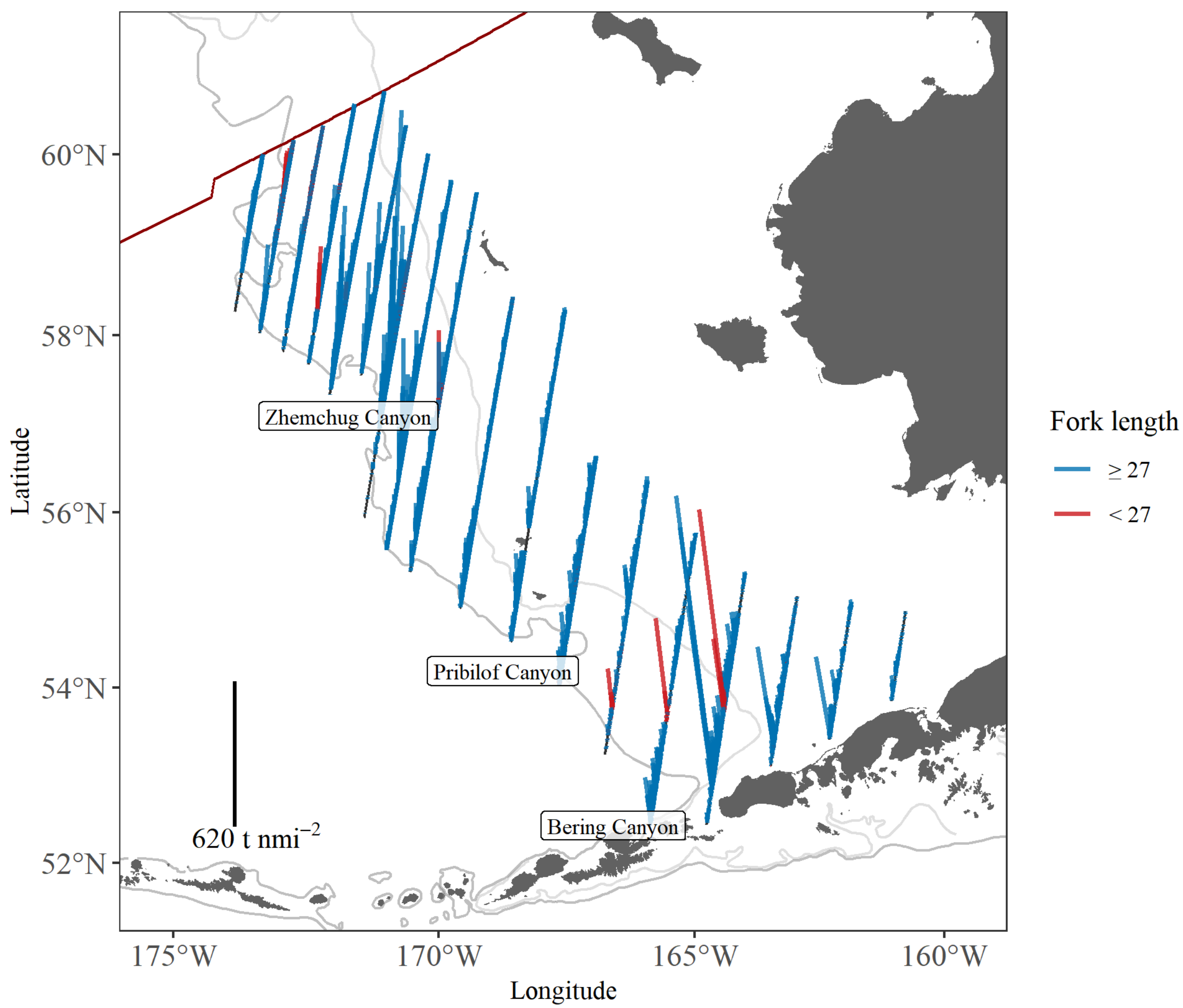

Figure 7. -- Biomass (t nmi^{-2}) attributed to pollock (vertical lines) for pollock > 27 cm fork length and ≤ 27 cm fork length along tracklines surveyed during the summer 2024 EBS acoustic-trawl survey core area.

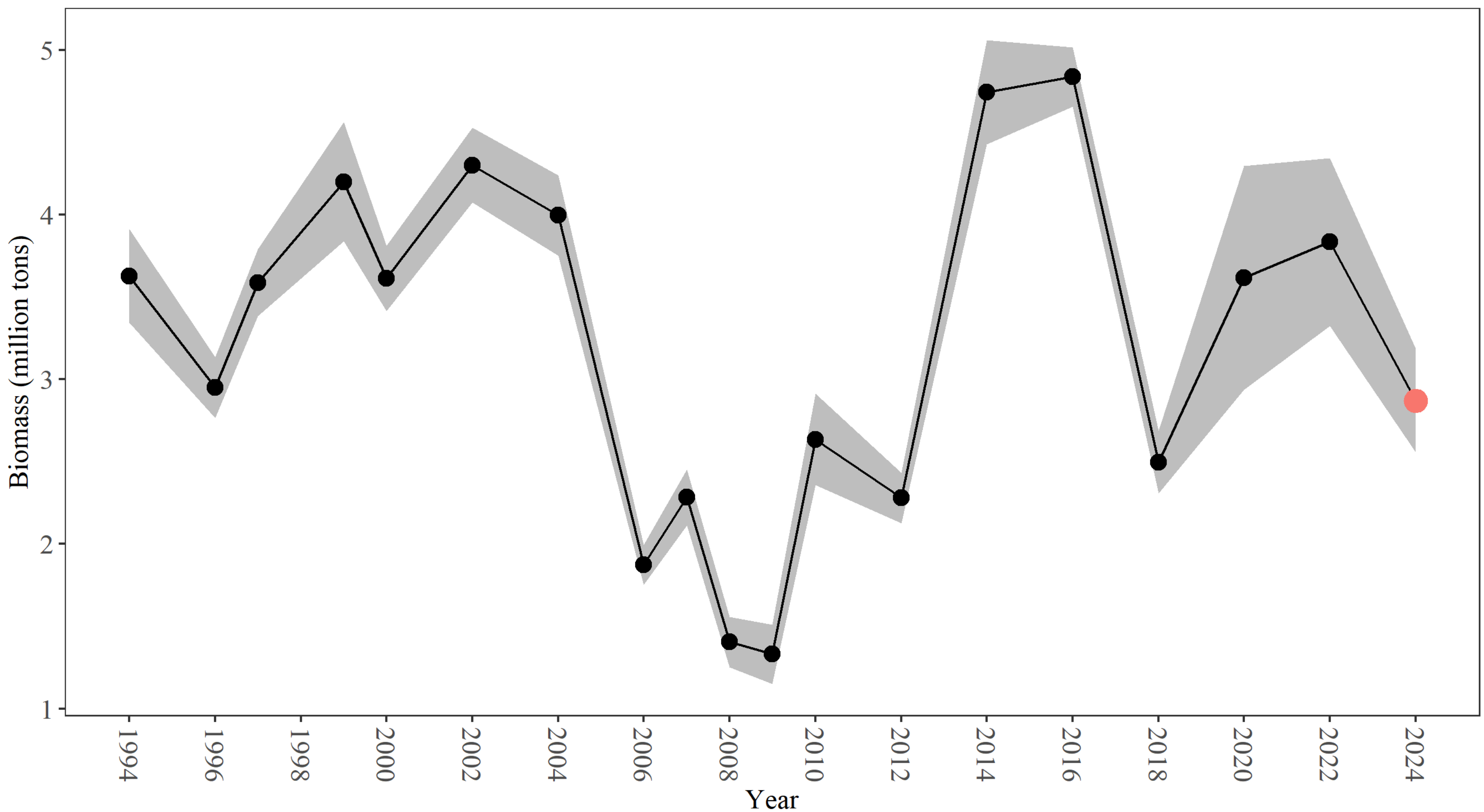

Figure 8. -- Summary of age-1+ pollock biomass estimates (millions of metric tons) for the EBS based on acoustic-trawl surveys from 1994 to 2024. Current survey estimate in red, and shaded area indicates 1-D geostatistical 95% confidence intervals from 1994 to 2024.

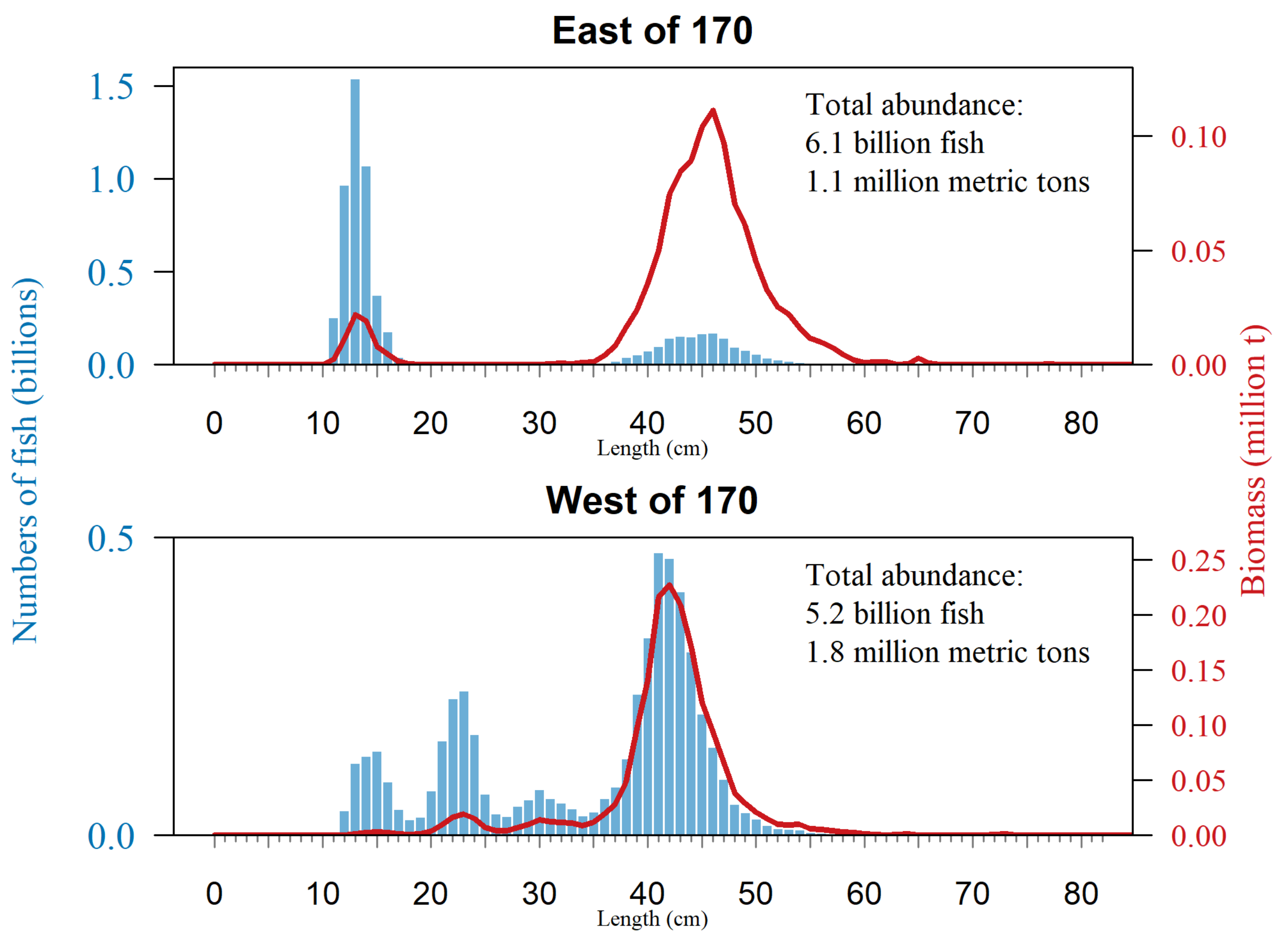

Figure 9. -- Pollock biomass (million metric tons; red line) and numbers (billion fish; blue bars) at length for the 2024 acoustic-trawl survey of the Eastern Bering Sea. This includes biomass and numbers at length from 16.0 m below the surface to 0.5 m above bottom.

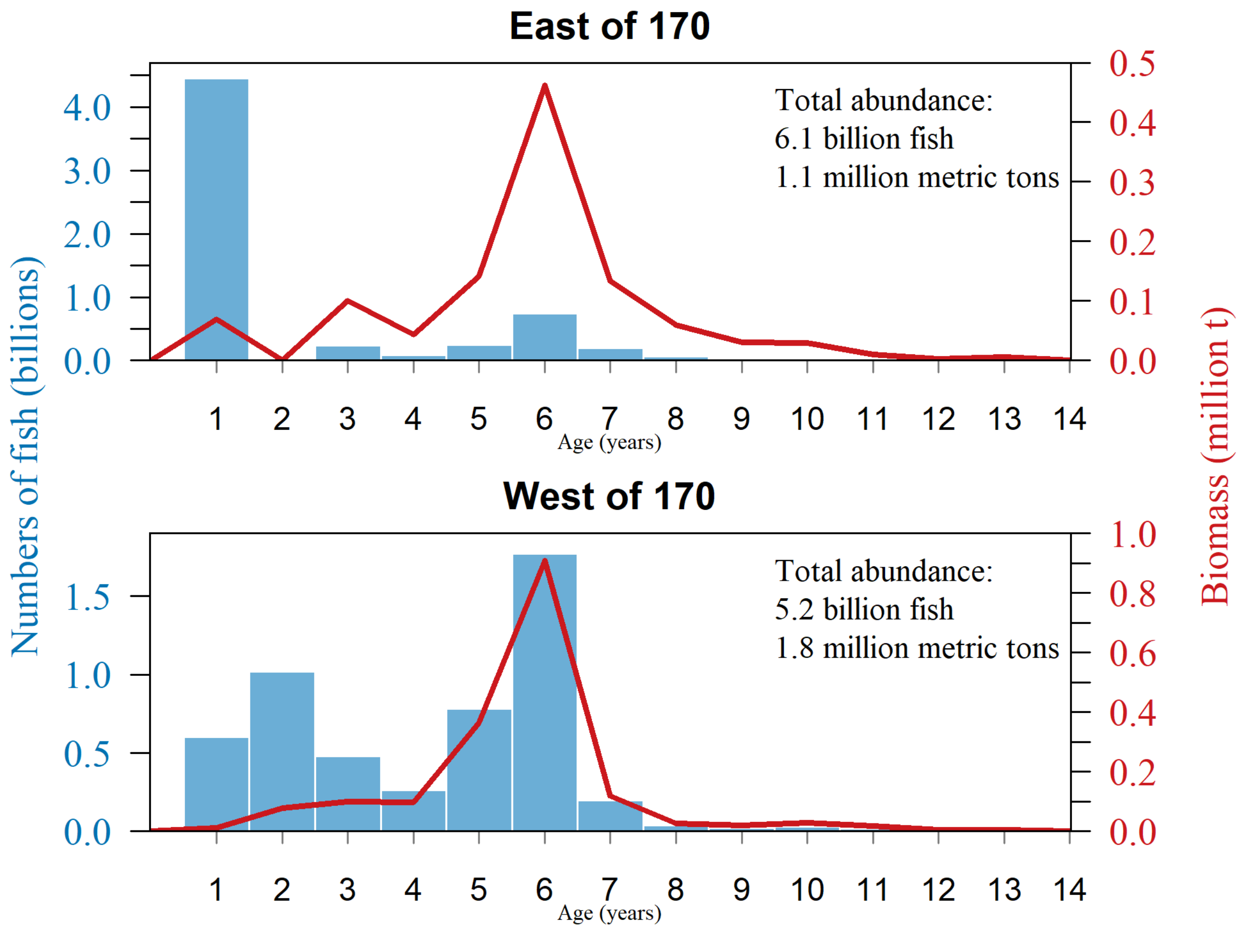

Figure 10. -- Pollock biomass (million metric tons; red line) and numbers (billion fish; blue bars) at age for the 2024 acoustic-trawl survey of the Eastern Bering Sea. This includes biomass and numbers at age down to 0.5 m off bottom.

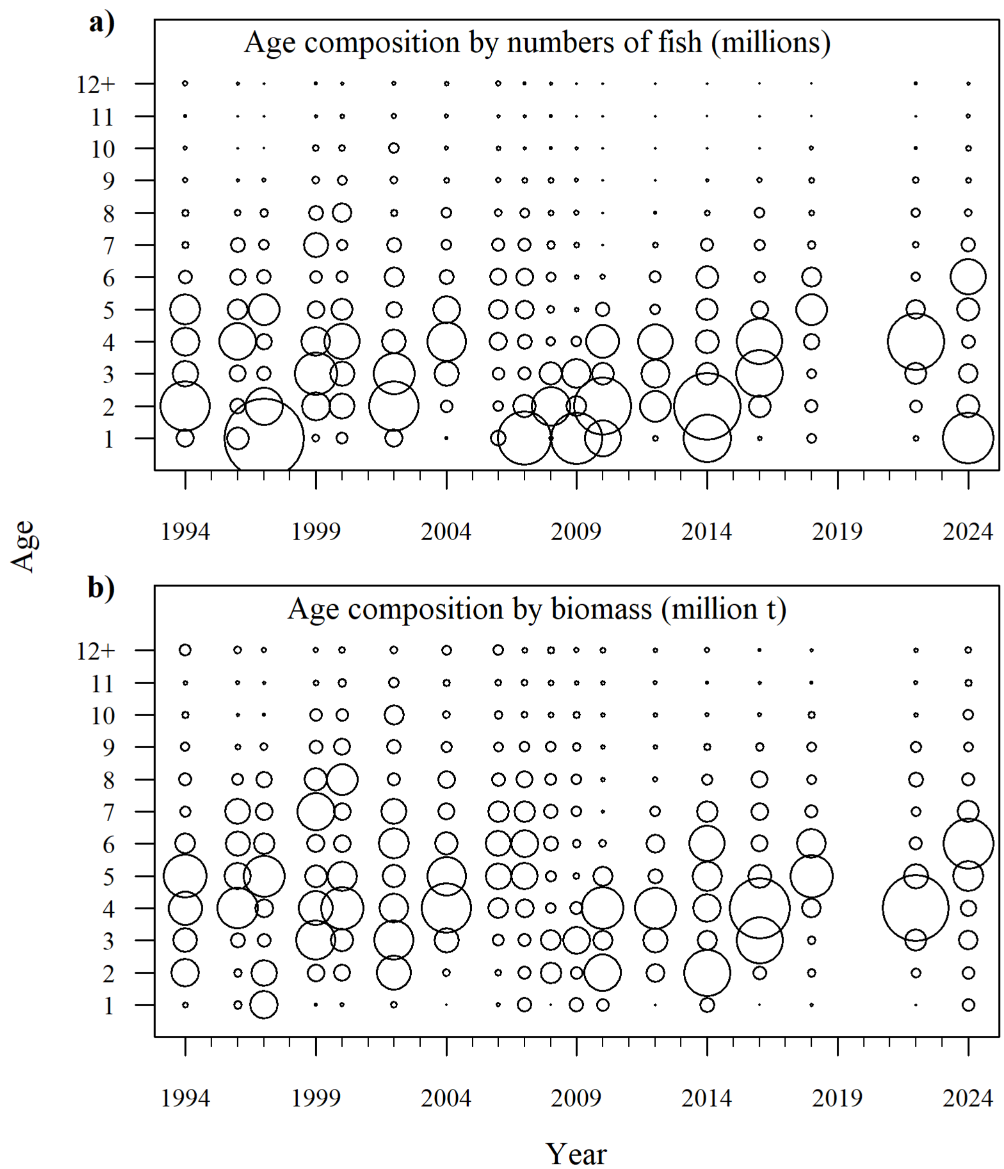

Figure 11. -- Historical numbers (a) and biomass (b) at age of walleye pollock between near surface and 0.5 m off bottom in the U.S. EEZ for summer Eastern Bering Sea acoustic-trawl surveys between 1994 and 2024.

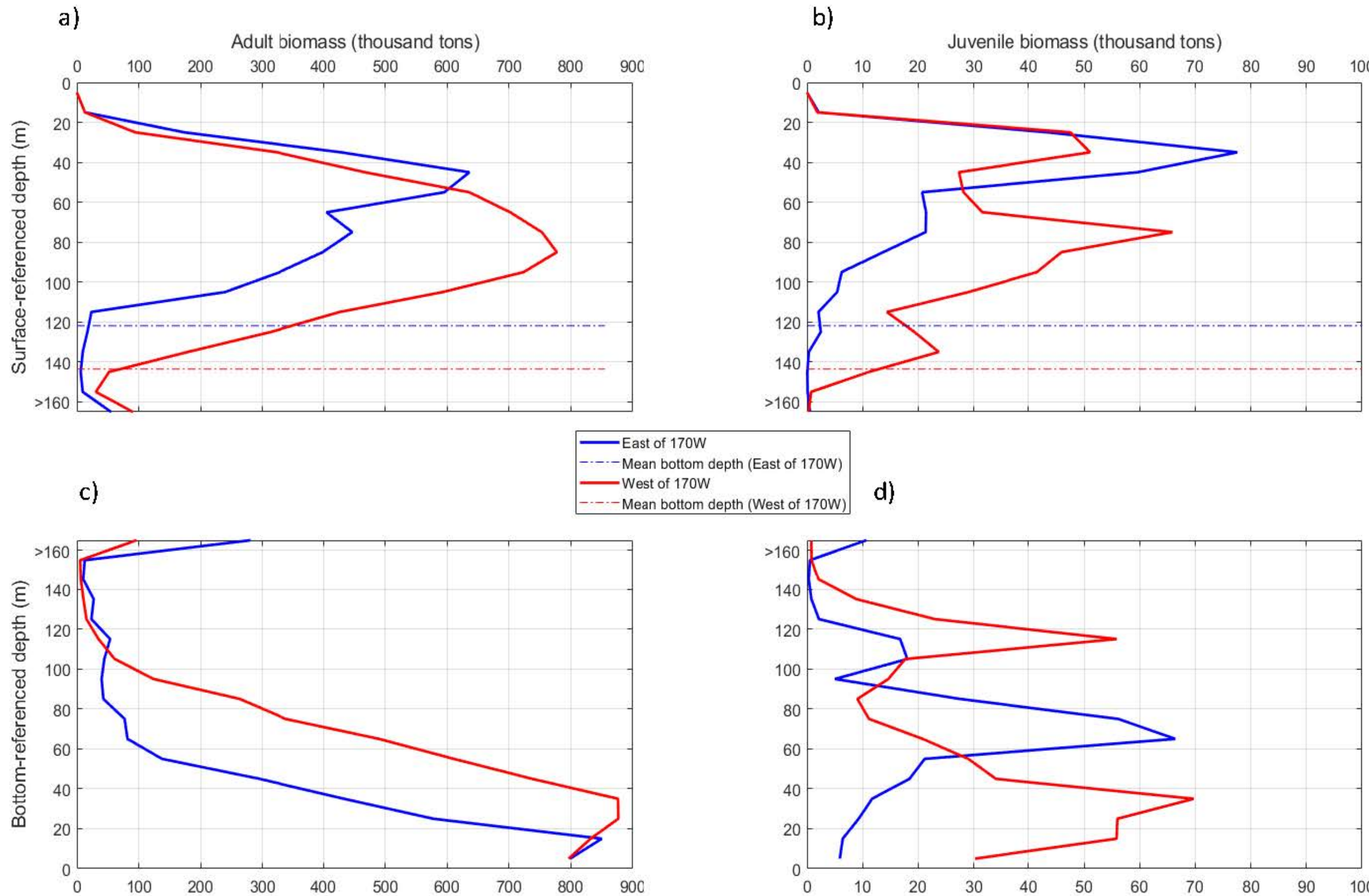

Figure 12. -- Depth distribution (m) of adult (≥ 30 cm FL; a & c) and juvenile (< 30 cm FL; b & d) walleye pollock biomass (thousand metric tons) east and west of 170°W longitude in the core survey area for the 2024 Eastern Bering Sea acoustic-trawl survey. Depth is referenced to the surface (a & b) and to the bottom (c & d). Data were averaged in 10 m depth bins from near surface to within 0.5 m of the seafloor.

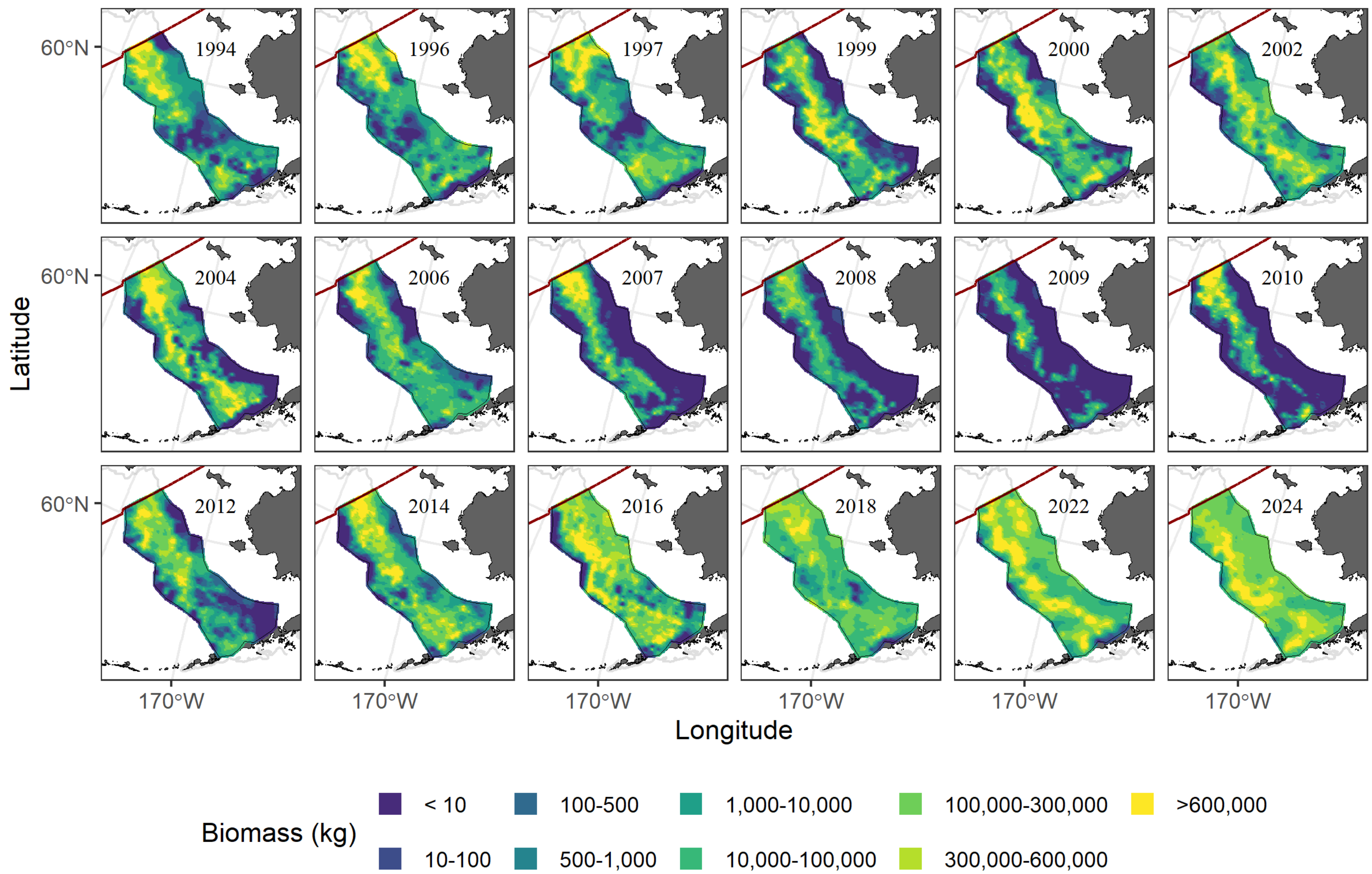

Figure 13. -- Historical pollock biomass between near surface and 3.0 m off bottom in the summer Eastern Bering Sea acoustic-trawl surveys of the U.S. EEZ between 2004 and 2024. Biomass between 3.0 m and the seafloor is not shown.

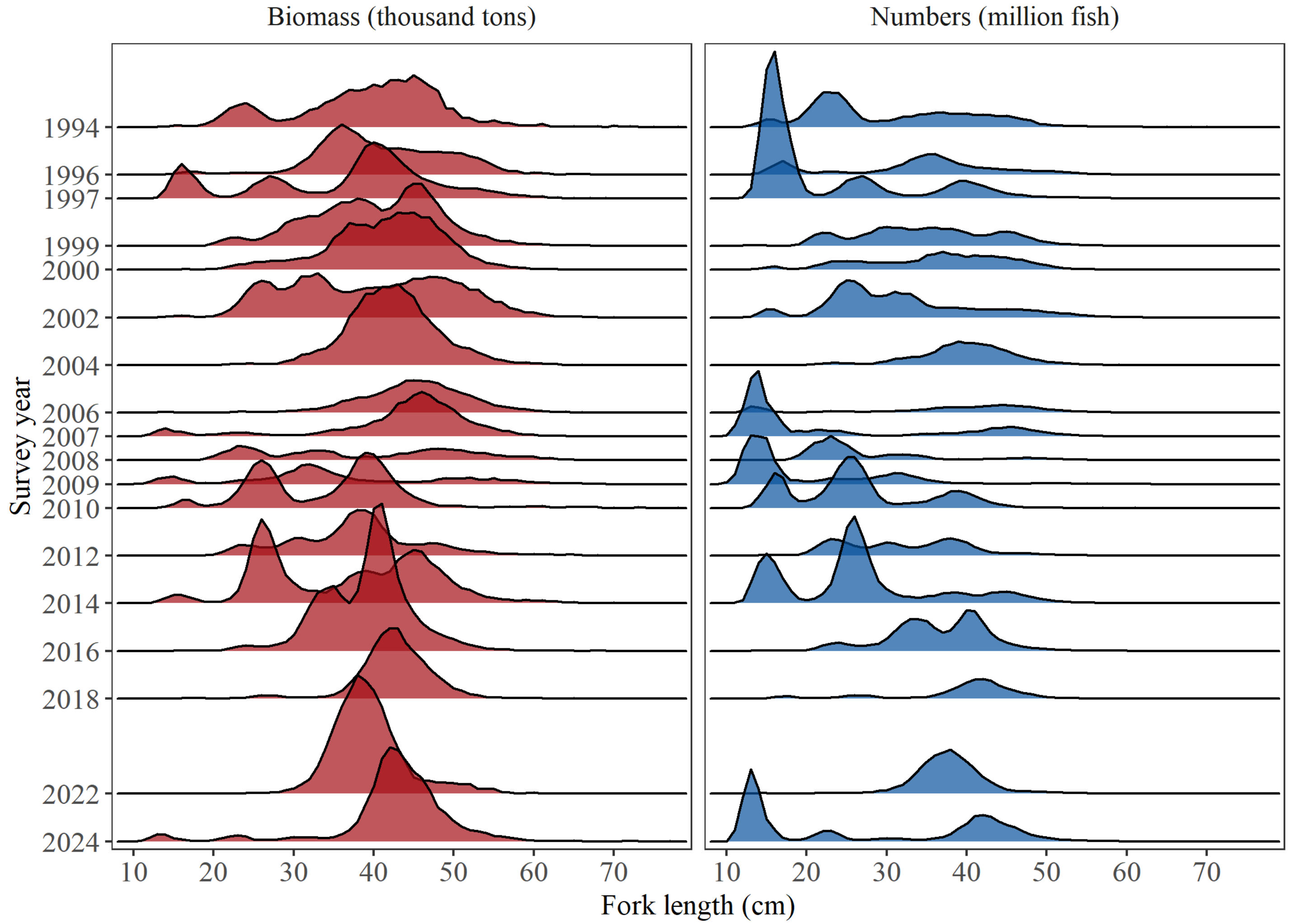

Figure 14. -- Time series of pollock population length composition by biomass (left panel) and numbers (right panel) from acoustic-trawl surveys of the Eastern Bering Sea core area from 1994 to 2024. The scale is the same for all years pictured.

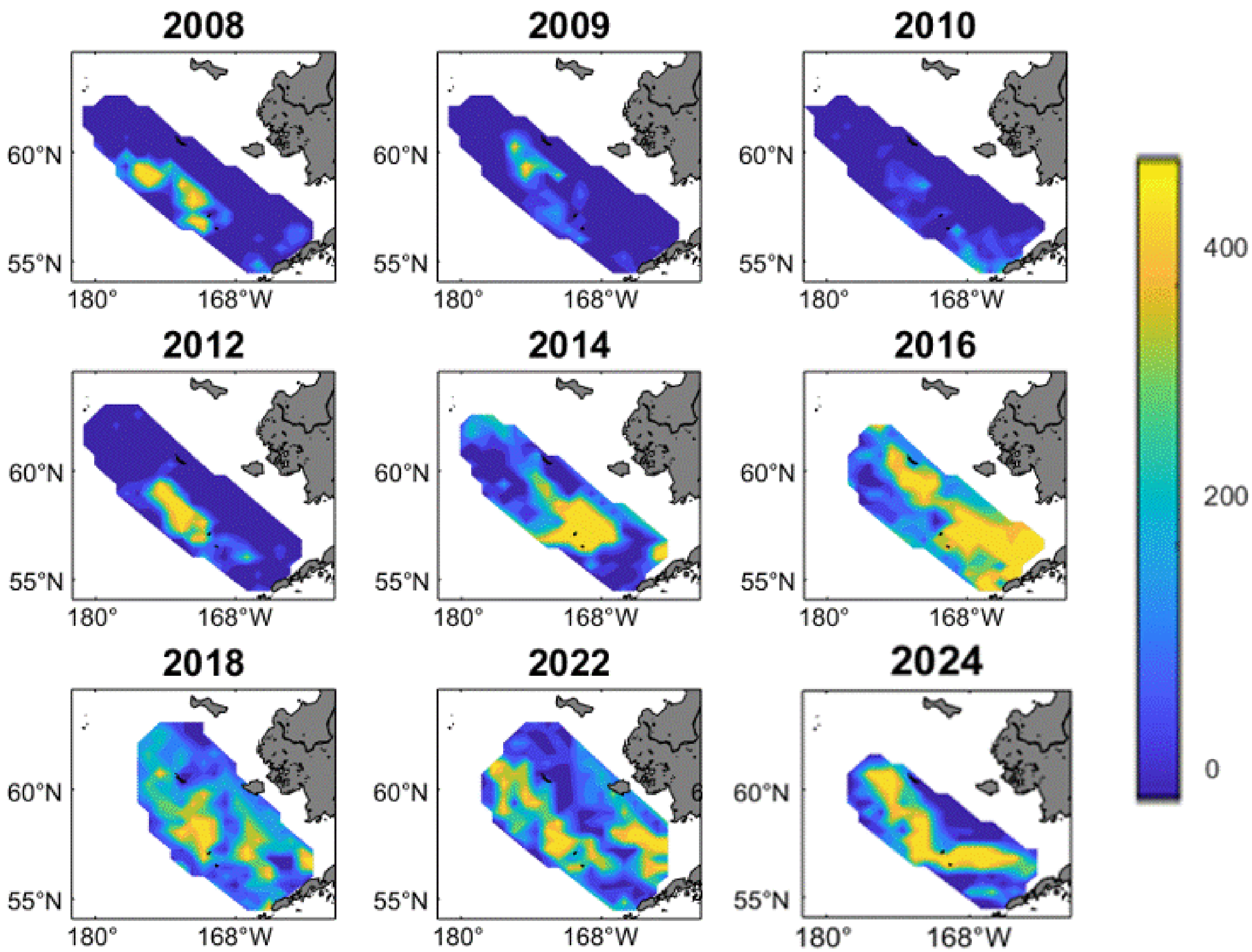

Figure 15. -- Backscatter attributed to a persistent non-walleye pollock, non-fish species mixture between near surface and 0.5 m off bottom, typically observed above the thermocline, in the U.S. EEZ for summer Eastern Bering Sea acoustic-trawl surveys between 2008 and 2024.

APPENDIX I. ITINERARY

Leg 1

5 June	Depart Dutch Harbor, AK
7 June	Acoustic sphere calibration in Kalsin Bay, Kodiak Island
7 June	In port Kodiak
9 June	Transit to survey start area
11 June-24 June	Acoustic-trawl survey of the EBS shelf (Transects 2-18)
25 June	Transit to Dutch
25 June-30 June	In port Dutch

Leg 2

30 June	Transit to survey resume point
1 July-11 July	Acoustic-trawl survey of the EBS shelf (Transects 18-28; westbound)
11 July-18 July	Acoustic-trawl survey of the EBS shelf (Transects 27-21; eastbound)
19 July	Acoustic sphere calibration in Makushin Bay, Unalaska Island
19 July	In Dutch Harbor, AK. End of survey

APPENDIX II. SCIENTIFIC PERSONNEL

Leg 1

Name	Position	Organization
Denise McKelvey	Chief Scientist	AFSC
Scott Furnish	Computer Spec.	AFSC
Matthew Phillips	Biologist	AFSC
Alex De Robertis	Biologist	AFSC
Darin Jones	Biologist	AFSC
Adam Spear	Biologist	AFSC
David Bryan	Biologist	AFSC
Hyungbeen Lee	Biologist	NIFS

Leg 2

Name	Position	Organization
Abigail McCarthy	Chief Scientist	AFSC
Taina Honkalehto	Biologist	AFSC
Nicholas Lee	Teacher at sea	CACPS
Mike Levine	Computer Spec.	AFSC
Robert Levine	Biologist	AFSC
Moses Lurbur	Biologist	AFSC
David McGowan	Biologist	AFSC
Matthew Phillips	Biologist	AFSC
Sarah Stienessen	Biologist	AFSC

APPENDIX III. ABUNDANCE CALCULATIONS

The abundance of target species was calculated by combining the echosounder measurements with size and species distributions from trawl catches and TS-length relationships from the literature (see De Robertis et al. 2017b for details). The echosounder measures volume backscattering strength, which is integrated vertically to produce the nautical area scattering coefficient, s_A (units of m^2 nmi^{-2}; MacLennan et al. 2002). The backscatter from an individual fish of species s at length l is referred to as its backscattering cross-section, $\sigma_{bs_{s,l}}$ (m^2), or in logarithmic terms as its target strength, $TS_{s,l}$ (dB re 1 m^2):

$$TS_{s,l} = 10\log_{10}\left(\sigma_{bs_{s,l}}\right) . \qquad \text{(Eq. } i\text{)}$$

The numbers of individuals of species s in length class l ($N_{s,l}$) captured in the nearest haul h were used to compute the proportion of acoustic backscatter associated with each species and length. First, the number of individuals in the catch were converted to a proportion ($P_{s.l,h}$):

$$P_{s,l,h} = \frac{N_{s,l,h}}{\sum_{s,l} N_{s,l,h}} \ , \quad \text{where} \sum_{s,l} P_{s,l,h} = 1 \ . \qquad \text{(Eq. } ii\text{)}$$

In analyses where trawl selectivity was considered, the selectivity-corrected numbers $N_{s_{corr},l,h}$ were used in place of $N_{s,l,h}$ in Eq. ii. This correction corrects the catch for trawl escapement. The corrected catch is that expected for an unselective sampling device. Refer to the main text for a description of the selectivity corrections applied.

The mean backscattering cross-section (an areal measure of acoustic scattering in m^2; MacLennan et al 2002) of species s of length class l is:

$$\sigma_{bs_{s,l}} = 10^{(0.1 \cdot TS_{s,l})} \ , \qquad \text{(Eq. } iii\text{)}$$

where TS is the target strength (dB re 1 m^2) of species s at size l (Table 2).

The proportion of backscatter from species s of length class l in haul h ($PB_{s,l,h}$) is computed from the proportion of individuals of species s and length class l estimated from haul h ($P_{s,l,h}$) and their backscattering cross-section:

$$PB_{s,l,h} = \frac{P_{s,l,h} \cdot \sigma_{bs_{s,l}}}{\sum_{s,l}\left(P_{s,l,h} \cdot \sigma_{bs_{s,l}}\right)} \ . \qquad \text{(Eq. } iv\text{)}$$

The measured nautical area scattering coefficient (s_A) at interval i was allocated to species s and length l as follows:

$$s_{A_{s,l,i}} = s_{A_i} \cdot PB_{s,l,h} \ , \qquad \text{(Eq. } v\text{)}$$

where haul h is the nearest haul within a stratum assigned to represent the species composition in a given 0.5 nmi along-track interval i. The nearest geographic haul was determined by using the great-circle distance to find the nearest trawl location (defined as the location where the net is at depth and begins to catch fish) out of the pool of hauls assigned to the same stratum (see above for details) closest to the start of interval i.

The abundance of species of length l in an area encompassing a series of transect intervals i was estimated from the area represented by that interval (A_i, nmi^2), the mean areal backscatter attributed to species s in given length/size class l ($s_{A_{s,l,i}}$, m^2 nmi^{-2}), and mean backscattering cross-section of species s at that size ($\sigma_{bs_{s,l}}$ m^2) as follows:

$$\text{Numbers-at-length } l\text{: } N_{s,l} = \sum_i \left(\frac{s_{A_{s,l,i}}}{4\pi\sigma_{bs_{s,l,i}}} \times A_i \right) \qquad \text{(Eq. } vi\text{)}$$

$$\text{Biomass-at-length } l\text{: } B_{s,l} = \sum_i \left(W_{s,l} \times N_{s,l,i} \right) \ , \qquad \text{(Eq. } vii\text{)}$$

where $W_{s,l}$ is the mean weight-at-length for species s in each 1-cm length l derived from length-weight regressions. In the case of pollock, when five or more individuals were measured within a length interval, the mean weight-at-length was used. Otherwise (i.e., for length classes of pollock with < 5 weight measurements, or other species), weight-at-length was estimated using a linear regression of the natural log-transformed length-weight data (De Robertis and Williams 2008).

The abundance-at-age was computed from $Q_{s,l,j}$, the proportion of j-aged individuals of species s in length class l, and the abundance of that species and age class in each surveyed interval follows:

$$\text{Numbers-at-age } j: N_{s,j} = \sum_{i} \left(Q_{s,l,j} \times N_{s,l} \right) \qquad \text{(Eq. } viii\text{)}$$

$$\text{Biomass-at-age } j: B_{s,j} = \sum_{i} \left(Q_{s,l,j} \times B_{s,l} \right) \ . \qquad \text{(Eq. } ix\text{)}$$

APPENDIX IV. EFFECT OF REDUCED SAMPLING RESOLUTION AND ALTERED SURVEY TIMING

The 2024 survey was conducted at a lower resolution and with different timing than in the past. We briefly summarize some relevant previous work, report a comparative analysis, and engage in some informed speculation about the impacts of these survey modifications on 2024 results.

An initial comparison of the complete survey presented in this report (which included 20 nmi spacing in the NW survey area and 40 nmi spacing elsewhere, see Methods section and Figure 7 for details) was made with a survey analysis using only the even survey transects spaced at 40 nmi. This suggested that the analysis of just the 40 nmi-spaced transects under-sampled smaller pollock (10-20 cm, typical of age-1 fish), resulting in a -0.26% reduction in survey numbers, a 5.69% increase in weight, and an increase in coefficient of variance (CV) from 5.6% to 5.9% (Fig. A4.1): more acoustic backscatter was attributed to larger fish.

These relatively small differences prompted further analysis of the NW part of the survey (Fig. A4.2), in which we assessed the impact of surveying just the even-numbered transects at 40 nmi spacing ("first pass"), just the odd-numbered transects at 40 nmi spacing ("second pass"), or all of the data collected at 20 nmi spacing ("full data set"). The lost survey days meant that fewer transects and fewer trawls were completed, and that the survey was completed earlier in the summer. We compared the uncertainty in our results using a 1-D estimate of variance (EVA) method (Petitgas 1993).

Pollock Abundance and Distribution

Fewer transects

There were 30% fewer survey transects in 2024 than in a typical survey, and they were farther apart; 40 nmi spacing for transects 2-20 and 20 nmi spacing for transects 21-28 (Fig. A4.2). With more widely spaced transects, each sample is extrapolated farther. By the definition of the 1-D geostatistical relative estimation errors for our survey estimates, variance will increase proportionately to transect spacing: given the same variogram model, if spacing increases 2×, so does variance, and CV increases by 1.4× (Petitgas 1993). Analysis of past EBS surveys shows that in practice, CV increases by about 2× when odd or even transects are analyzed separately (resulting in 2× transect spacing; De Robertis, et al. 2021). The maximum transect spacing for optimal precision and distribution is approximately 30 nmi (Walline 2007, Stienessen et al. 2025). As noted in the main report text, the CV of survey biomass calculated using all the available data was within the range of past surveys, so the increase in spatial sampling uncertainty resulting from fewer transects may have been modest.

Fewer trawls

1-D geostatistical relative estimation error only includes spatial sampling error (patchiness) from the transect data. If fewer trawls are done, sampling of the species, length, and age composition is also reduced, which isn't explicitly included in that error estimate. Levine et al. (2021, Appendix I) simulated the effect of reduced trawling effort in past summer Gulf of Alaska pollock surveys, which suggested that, for 25-50% reductions in trawling in the simulations, CVs were 2-15% higher, but the point estimates stayed within about 5% of the average. Larger differences were observed when multiple size modes were present in the survey, which was true of the 2024 summer EBS survey. The effect of fewer trawls on summer EBS surveys may be smaller than for the summer Gulf of Alaska surveys because the species composition is less variable. However, the length composition of this year's EBS survey was somewhat more variable (multiple length modes) than typical. We can speculate that the increase in survey uncertainty due to fewer trawls may have been small, and had more impact on estimates of the patchily distributed juvenile age classes.

Survey completed earlier, transects executed in a different order

Most EBS acoustic-trawl surveys begin in late May/early June and end in early/mid-August, working from east to west. In 2024, the survey ended earlier than usual, and additional transects and trawling were added at the end, from west to east, with those later trawls and transects sampled out of the usual sequence (Appendix I). Spatial, temporal, and spatiotemporal effects on sampling are difficult to estimate with these data and the limited number of existing studies in the literature. Comparisons of pollock backscatter from EBS bottom trawl Acoustic Vessel of Opportunity (AVO) surveys and acoustic-trawl surveys with lags in sampling time of a few weeks show broad agreement at the shelf-scale, but differences in fine-scale patterns (Honkalehto et al. 2011). Levine et al. (2024) reported measurements of pollock flux from a series of acoustic echosounder moorings across the western EBS shelf suggesting that rates of directed fish movement are low in summer. Finally, Stienessen et al. (2025) reported on cross-transect data gathered at end of the summer 2022 EBS acoustic-trawl survey that suggested spatial patterns of pollock were generally consistent on the western shelf over a period of a few weeks. Taken together, all this suggests that large-scale spatial patterns of pollock were likely stable on the timescale of the 2024 survey execution.

Comparative analyses of survey results

Spatial, temporal, and spatiotemporal sources of variability are not easily separated in this dataset. However, additional analysis can contribute some further information about the temporal and spatial stability of survey results.

When we examined only the area in which there was variable transect spacing, transects 21-28 of the NW portion of the EBS survey, the potential effect of coarser sampling became clearer (Figs. A4.2 and A4.3). Since trawls done on the first pass of 40 nmi-spaced transects (even transects 22-28) did not capture as many age-1 pollock (modal fork length 15 cm) as the second pass (odd transects 21-27) or the full data set, more acoustic backscatter was attributed to larger fish (compare solid blue and dashed blue lines in left panel of A4.3). The CV for the first pass (15.5%) was higher than for the second pass (11.7%). When all transects were used, the length-frequency composition and biomass and abundance estimates were intermediate between the first- and second-pass estimates, and the CV was lower (7.1%; Fig. A4.3).

Generally, these results are consistent with our past observations on the impacts of fewer transects and fewer trawls. We can speculate that the effects of reduced precision and altered survey timing were relatively small for this survey, with the most added uncertainty due to estimation of the abundance and distribution of juvenile age-classes. The effect on the survey estimate would have been greater if the distribution of juvenile fishes had been more restricted, as it occasionally has been in past EBS surveys, particularly relative to the distribution of larger pollock.

Water Temperature

Surface temperature results may have been affected by the relatively early timing and shorter duration of the 2024 survey, as seasonal warming of surface waters typically leads to maximum SST in August (Overland et al. 1999), and the 2024 survey ended about 3 weeks earlier than usual on 18 July. A typical survey extending into August would likely have encountered some warmer surface temperatures. Bottom temperatures are less likely to be impacted by survey timing as they are driven more by sea ice extent in the prior winter (Wyllie-Echeverria and Wooster 1998).

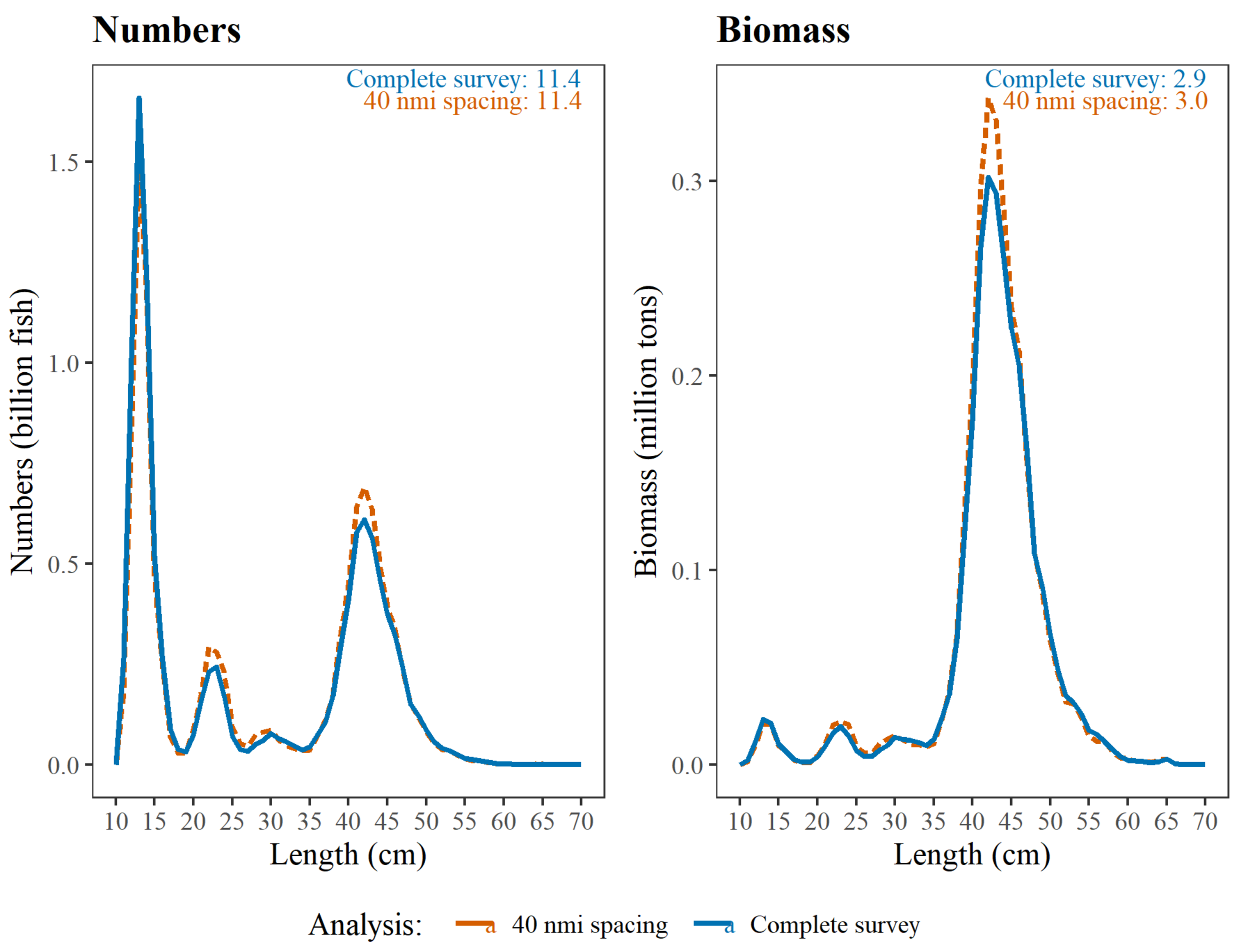

Figure A4.1. -- Biomass and numbers of pollock at length for the 2024 EBS acoustic-trawl survey. The blue lines represent mixed 20/40 nmi spacing, using all the available survey data, and the orange dashed lines show 40 nmi spacing leaving out the transects surveyed from west to east.

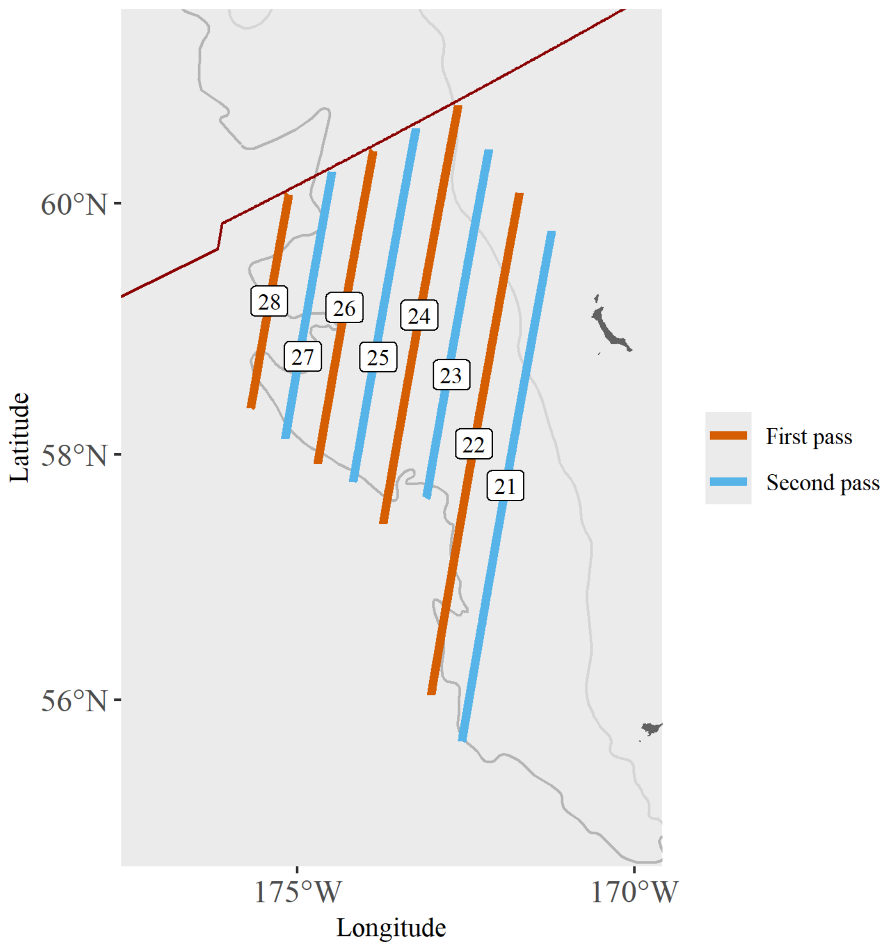

Figure A4.2. -- Transect lines from the northwestern component of the 2024 Eastern Bering Sea acoustic-trawl survey. The data set associated with each transect is indicated by the transect color. The U.S.-Russia Convention line is shown in dark red.

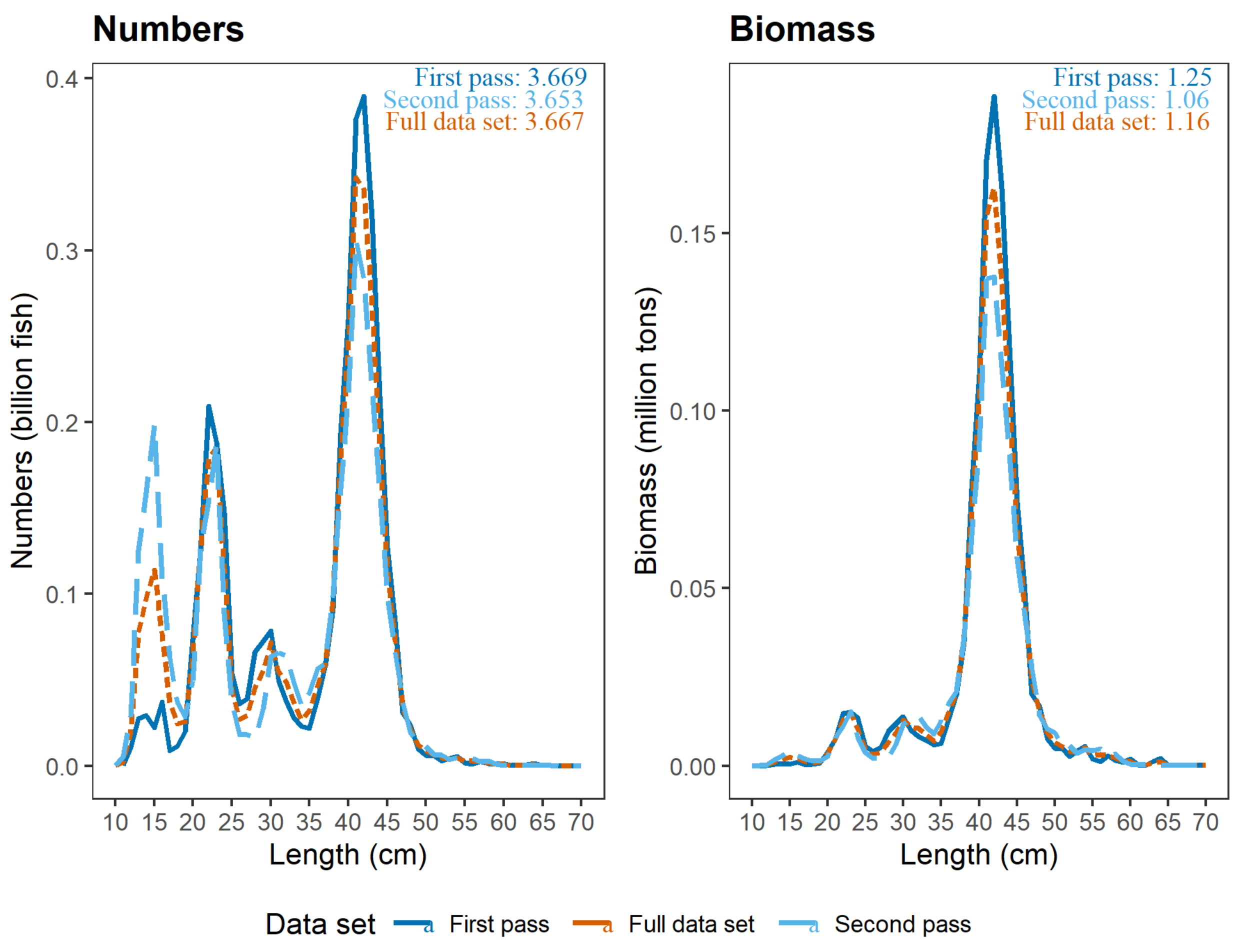

Figure A4.3. -- Comparison of three different subsets of the data from the NW area of the 2024 EBS acoustic-trawl survey. The "first pass" is the even transects at 40 nmi spacing, "second pass" is just the odd transects at 40 nmi spacing, and the full data set is all of the transects, with 20 nmi spacing.

CITATIONS

Bodholt, H. 2002. The effect of water temperature and salinity on echo sounder measurements. ICES Symposium on Acoustics in Fisheries, Montpellier, France, 10–14 June 2002.

Bodholt, H., and H. Solli. 1992. Split beam techniques used in Simrad EK500 to measure target strength. Pages 16–31 *In* World Fisheries Congress. May 1992, Athens, Greece.

De Robertis, A., M. Levine, N. Lauffenburger, T. Honkalehto, J. Ianelli, C. Monnahan, R. Towler, D. Jones, S. Stienessen, and D. McKelvey. 2021. Uncrewed surface vehicle (USV) survey of walleye pollock, *Gadus chalcogrammus*, in response to the cancellation of ship-based surveys. ICES J. Mar. Sci. 78:2797–2808.

De Robertis, A., D. R. McKelvey, and P. H. Ressler. 2010. Development and application of an empirical multifrequency method for backscatter classification. Can. J. Fish. Aquat. Sci. 67:1459–1474.

De Robertis, A., and K. Taylor. 2014. *In situ* target strength measurements of the scyphomedusa *Chrysaora melanaster*. Fish. Res. 153:18–23.

De Robertis, A., K. Taylor, K. Williams, and C. D. Wilson. 2017a. Species and size selectivity of two midwater trawls used in an acoustic survey of the Alaska Arctic. Deep Sea Res. Pt. II 135:40–50.

De Robertis, A., K. Taylor, C. D. Wilson, and E. V. Farley. 2017b. Abundance and distribution of Arctic cod (*Boreogadus saida*) and other pelagic fishes over the U.S. Continental Shelf of the Northern Bering and Chukchi Seas. Deep Sea Res. Part II 135:51–65.

De Robertis, A., and K. Williams. 2008. Weight-length relationships in fisheries studies: The standard allometric model should be applied with caution. Trans. Am. Fish. Soc. 137:707–719.

Demer, D. A., L. Berger, M. Bernasconi, E. Bethke, K. Boswell, D. Chu, R. Domokos, A. Dunford, S. Fässler, S. Gauthier, L. T. Hufnagle, J. M. Jech, N. Bouffant, A. Lebourges-Dhaussy, X. Lurton, G. J. Macaulay, Y. Perrot, T. Ryan, S. Parker-Stetter, S. Stienessen, T. Weber, and N. Williamson. 2015. Calibration of acoustic instruments. ICES Coop. Res. Rep. 326. 133 p.

Demer, D. A., and S. G. Conti. 2005. New target-strength model indicates more krill in the Southern Ocean. ICES J. Mar. Sci. 62:25–32.

Foote, K. G. 1987. Fish target strengths for use in echo integrator surveys. J. Acoust. Soc. Am. 82:981–987.

Foote, K. G., H. P. Knudson, G. Vestnes, and E. J. Simmonds. 1987. Calibration of acoustic instruments for fish density estimation: A practical guide. ICES Coop. Res. Rep. 144:69.

Foote, K. G., and J. J. Traynor. 1988. Comparisons of walleye pollock target strength estimates determined from *in situ* measurements and calculations based on swimbladder form. J. Acoust. Soc. Am. 83:9–17.

Gauthier, S., and J. K. Horne. 2004. Acoustic characteristics of forage fish species in the Gulf of Alaska and Bering Sea based on Kirchhoff-approximation models. Can. J. Fish. Aquat. Sci. 61:1839–1850.

Guttormsen, M. A., and C. D. Wilson. 2009. *In situ* measurements of capelin (*Mallotus villosus*) target strength in the North Pacific Ocean. ICES J. Mar. Sci. 66:258–263.

Honkalehto, T., and A. McCarthy. 2015. Results of the acoustic-trawl survey of walleye pollock ((*Gadus chalcogrammus*) on the U.S. and Russian Bering Sea shelf in June - August 2014 (DY1407). AFSC Processed Rep. 2015-02, Alaska Fish. Sci. Cent., NOAA, Natl. Mar. Fish. Serv., 7600 Sand Point Way NE, Seattle WA 98115:61 p.

Honkalehto, T., A. McCarthy, and N. Lauffenburger. 2018. Results of the acoustic-trawl survey of walleye pollock (*Gadus chalcogrammus*) on the U.S. Bering Sea shelf in June - August 2016 (DY1608). AFSC Processed Rep. 2018-03, 78 p. Alaska Fish. Sci. Cent., NOAA, Natl. Mar. Fish. Serv., 7600 Sand Point Way NE, Seattle WA 98115:78 p.

Honkalehto, T., A. McCarthy, M. Levine, D. Jones, and K. Williams. 2022. Results of the acoustic-trawl survey of walleye pollock (*Gadus chalcogrammus*) in Shelikof Strait and Marmot Bay March 2021 (DY-202102). AFSC Processed Rep. 2022-08, 78 p. Alaska Fish. Sci. Cent., NOAA, Natl. Mar. Fish. Serv., 7600 Sand Point Way NE, Seattle WA 98115:78 p.

Honkalehto, T., A. McCarthy, P. Ressler, and D. Jones. 2013. Results of the acoustic-trawl survey of walleye pollock (*Theragra chalcogramma*) on the U.S. and Russian Bering Sea shelf in June - August (DY1207). AFSC Processed Rep. 2013-02, 60 p. Alaska Fish. Sci. Cent., NOAA, Natl. Mar. Fish. Serv., 7600 Sand Point Way NE, Seattle WA 98115:60 p.

Honkalehto, T., A. McCarthy, P. Ressler, D. Jones, and K. Williams. 2012. Results of the acoustic-trawl survey of walleye pollock (*Theragra chalcogramma*) on the U.S. and Russian Bering Sea shelf in June - August 2010 (DY1006). AFSC Processed Rep. 2012-01, 57 p. Alaska Fish. Sci. Cent., NOAA, Natl. Mar. Fish. Serv., 7600 Sand Point Way NE, Seattle WA 98115:57 p.

Honkalehto, T., P. H. Ressler, R. Towler, and C. D. Wilson. 2011. Using acoustic data from fishing vessels to estimate walleye pollock abundance in the eastern Bering Sea. Can. J. Fish. Aquat. Sci.:1231–1242.

Jech, J. M., K. G. Foote, D. Chu, and L. C. Hufnagle. 2005. Comparing two 38-kHz scientific echosounders. ICES J. Mar. Sci. 62:1168–1179.

Jones, D. T., A. De Robertis, and N. J. Williamson. 2011. Statistical combination of multi-frequency sounder-detected bottom lines reduces bottom integrations. U.S. Dep. Commer., NOAA Tech. Memo. NMFS-AFSC-219:13 p.

Jones, D. T., N. E. Lauffenburger, K. Williams, and A. De Robertis. 2019. Results of the acoustic-trawl survey of walleye pollock (*Gadus chalcogrammus*) in the Gulf of Alaska, June-August 2017 (DY2017-06). AFSC Processed Rep. 2019-08, 110 p. Alaska Fish. Sci. Cent., NOAA, Natl. Mar. Fish. Serv., 7600 Sand Point Way NE, Seattle WA 98115.

Kang, D., T. Mukai, K. Iida, D. Hwang, and J.-G. Myoung. 2005. The influence of tilt angle on the acoustic target strength of the Japanese common squid (*Todarodes pacificus*). ICES J. Mar. Sci. 62:779–789.

Lauffenburger, N., A. De Robertis, and S. Kotwicki. 2017. Combining bottom trawls and acoustics in a diverse semipelagic environment: What is the contribution of walleye pollock (*Gadus chalcogrammus*) to near-bottom acoustic backscatter in the eastern Bering Sea? Can. J. Fish. Aquat. Sci. 74:256–264.

Levine, M., D. Jones, and D. McGowan. 2024. Results of the acoustic-trawl survey of walleye pollock (*Gadus chalcogrammus*) in the Gulf of Alaska, June-July 2021 (DY2021-04). AFSC Processed Rep. 2024-07, 100 p. Alaska Fish. Sci. Cent., NOAA, Natl. Mar. Fish. Serv., 7600 Sand Point Way NE, Seattle WA 98115.

Levine, M., and P. Ressler. 2024. Eastern Bering Sea Euphausiids ("Krill"), pp. 102-104. *In* Siddon, E. (Ed.), Ecosystem Status Report 2024: Eastern Bering Sea, Stock Assessment and Fishery Evaluation Report. North Pacific Fishery Management Council, 1007 West 3rd Ave., Suite 400, L92 Building, 4th floor, Anchorage, AK 99501.

MacLennan, D. N., P. G. Fernandes, and J. Dalen. 2002. A consistent approach to definitions and symbols in fisheries acoustics. ICES J. Mar. Sci. 59:365–369.

Markowitz, E. H., E. J. Dawson, C. B. Anderson, S. K. Rohan, N. E. Charriere, B. K. Prohaska, and D. E. Stevenson. 2023. Results of the 2022 eastern and northern Bering Sea continental shelf bottom trawl survey of groundfish and invertebrate fauna. U.S. Dep. Commer., NOAA Tech. Memo. NMFS-AFSC-469, 213 p. Alaska Fish. Sci. Cent., NOAA, Natl. Mar. Fish. Serv., 7600 Sand Point Way NE, Seattle WA 98115.

McCarthy, A., T. Honkalehto, N. Lauffenburger, and A. De Robertis. 2020. Results of the acoustic-trawl survey of walleye pollock (*Gadus chalcogrammus*) on the U.S. Bering Sea shelf in June - August 2018 (DY1807). AFSC Processed Rep. 2020-07, 83 p. Alaska Fish. Sci. Cent., NOAA, Natl. Mar. Fish. Serv., 7600 Sand Point Way NE, Seattle WA 98115.

Methot, R. D. 1986. Frame trawl for sampling pelagic juvenile fish. Calif. Coop. Oceanic. Fish. Invest. Rep 27:267–278.

Miller, D. M. 1984. Reducing transformation bias in curve fitting. Am. Stat. 38:124–126.

Ona, E. 2003. An expanded target-strength relationship for herring. ICES J. Mar. Sci. 60:493–499.

Ona, E., and R. B. Mitson. 1996. Acoustic sampling and signal processing near the seabed: The deadzone revisited. ICES J. Mar. Sci. 53:677–690.

Overland, J. E., S. A. Salo, L. H. Kantha, and C. A. Clayson. 1999. Thermal stratification and mixing on the Bering Sea shelf in Dynamics of the Bering Sea: A summary of physical, chemical and biological characteristics and a synopsis of research on the Bering Sea. Page 840. North Pacific Marine Science Organization (PICES),; University of Alaska Sea Grant College Program AK-SG-99-03, Sydney, British Columbia; Fairbanks, Alaska.

Pebesma, E. J. 2004. Multivariable geostatistics in S: The gstat package. Comp. & Geosci. 30:683–691.

Petitgas, P. 1993. Geostatistics for fish stock assessments: A review and an acoustic application. ICES J. Mar. Sci. 50:285–298.

Rivoirard, J., J. Simmonds, K. G. Foote, P. Fernandes, and N. Bez. 2000. Geostatistics for estimating fish abundance. 206 p. Blackwell Science Ltd, Oxford, UK.

Simmonds, E. J., and D. N. MacLennan. 2005. Fisheries acoustics: Theory and practice. 2nd edition. 473 p. Blackwell Science Ltd, Oxford, UK.

Simrad. 2018. Reference manual for Simrad EK80 scientific echo sounder application. Strandpromenenaden 50, Box 111, N-3191 Horten, Norway.

Stienessen, S., A. McCarthy, T. Honkalehto, N. Lauffenburger, and S. Urmy. 2025. Results of the acoustic-trawl survey of walleye pollock (*Gadus chalcogrammus*) on the U.S. Bering Sea Shelf in June-August 2022 (DY2207). AFSC Processed Rep. 2025-01, 68 p. Alaska Fish. Sci. Cent., NOAA, Natl. Mar. Fish. Serv., 7600 Sand Point Way NE, Seattle WA 98115.

Towler, R., and K. Williams. 2010. An inexpensive millimeter-accuracy electronic length measuring board. Fish. Res. 106:107–111.

Traynor, J. J. 1996. Target-strength measurements of walleye pollock (*Theragra chalcogramma*) and Pacific whiting (*Merluccius productus*). ICES J. Mar. Sci. 53:253–258.

Walline, P. D. 2007. Geostatistical simulations of eastern Bering Sea walleye pollock spatial distributions, to estimate sampling precision. ICES J. Mar. Sci. 64:559–569.

Williams, K., A. E. Punt, C. D. Wilson, and J. K. Horne. 2011. Length-selective retention of walleye pollock, *Theragra chalcogramma*, by midwater trawls. ICES J. Mar. Sci. 68:119–129.

Williams, K., C. N. Rooper, and R. Towler. 2010. Use of stereo camera systems for assessment of rockfish abundance in untrawlable areas and for recording pollock behavior during midwater trawls. Fish. Bull. U.S. 108:352–362.

Williams, K., R. Towler, P. Goddard, R. Wilborn, and C. Rooper. 2016. Sebastes Stereo Image Analysis Software. AFSC Processed Rep. 2016-03, 42 p. Alaska Fish. Sci. Cent., NOAA, Natl. Mar. Fish. Serv., 7600 Sand Point Way NE, Seattle WA 98115.

Williamson, N. J., and J. J. Traynor. 1996. Application of a one-dimensional geostatistical procedure to fisheries acoustic surveys of Alaskan pollock. ICES J. Mar. Sci. 53:423–428.

Wyllie-Echeverria, T., and W. S. Wooster. 1998. Year-to-year variations in Bering Sea ice cover and some consequences for fish distributions. Fish. Oceanogr. 7:159–170.

U.S. Secretary of Commerce
Howard Lutnick

Under Secretary of Commerce
for Oceans and Atmosphere and
NOAA Administrator
Neil Jacobs

Assistant Administrator, National
Marine Fisheries Service.
Eugenio Piñeiro Soler

January 2026

www.nmfs.noaa.gov

OFFICIAL BUSINESS

National Marine
Fisheries Service
Alaska Fisheries Science Center
7600 Sand Point Way N.E.
Seattle, WA 98115-6349